

MHD and thermal radiation effects in steady flow of nanofluids



By

Maria Imtiaz

Department of Mathematics
Quaid-i-Azam University
Islamabad, Pakistan
2012

MHD and thermal radiation effects in steady flow of nanofluids



By
Maria Imtiaz

A Dissertation Submitted in the Partial Fulfillment of the Requirements for
the
Degree of
MASTER OF PHILOSOPHY
IN

MATHEMATICS

Supervised By

Prof. Dr. Tasawar Hayat

Department of Mathematics
Quaid-i-Azam University
Islamabad, Pakistan
2012

MHD and thermal radiation effects in steady flow of nanofluids


By


Maria Imtiaz


CERTIFICATE

A DISSERTATION SUBMITTED IN THE PARTIAL FULFILLMENT OF THE REQUIREMENTS FOR THE DEGREE OF THE MASTER OF PHILOSOPHY

We accept this dissertation as conforming to the required standard

1. 
Prof. Dr. Muhammad Ayub
(Chairman)

2.  2/7/12
Prof. Dr. Tasawar Hayat
(Supervisor)

3. 
Prof. Dr. Akhtar Hussain
(External Examiner)

Department of Mathematics
Quaid-i-Azam University
Islamabad, Pakistan

Acknowledgement

*In the name of Allah, the most Merciful, the most Gracious. All praise is due to Allah; we praise Him, seek His help, and ask for His forgiveness. I am thankful to Allah, who supplied me with the courage, the guidance, and the love to complete this research. Also, I cannot forget the ideal man of the world and most respectable personality for whom Allah created the whole universe, **Prophet Muhammad (P. B. U. H)**.*

*My utmost appreciation and gratitude goes to my supervisor, **Prof. Dr. Tasawar Hayat** for his excellent guidance, constant encouragement, detailed comments, patience and care during the entire research of M.Phil. His truly scientist intuition has made me as a constant oasis of ideas and passions in science, which exceptionally inspire and enrich my growth as a student, a researcher and a scientist want to be.*

*I am thankful to Chairman, Department of Mathematics, **Prof. Dr. Muhammad Ayub**, for providing me proper atmosphere to complete the research work. Also the great contribution of my respected teachers particularly **Dr. Masud Khan, Dr. Sohail Nadeem** whose teaching have brought me to this stage of academic apex is highly acknowledged.*

*My heartfelt appreciation and gratefulness are dedicated to my **Parents**, sister **Fari**, brothers **Bilal** and **Hamza** and my niece **Minahil** for their constant prayers, guidance, encouragement and support throughout my career. They are the source of power, inspiration, and confidence in me.*

*I am indebted to my senior scholar **Mr. Zahid Iqbal**, I can say he is my co-supervisor with high respect and deep sense of appreciation for his expert and active involvement in each, experimental planning clearly, providing all necessary things to carry out research. I have also benefited by advice and guidance from all the members of **FMG** (Fluid Mechanics group) who always kindly granted me their suggestions and support. My sincere thanks are to my research fellows particularly **Farooq bhai** and **Sadia**.*

*My sincere and heartiest gratitude goes to my friends **Ayesha**, **Raana**, **Wajeeha**, **Rehana** and **Sumarna** who accompanied me on the bumpy road of life. I cherish our many days together during study in lawns, laughing in library, shopping in markets and enjoying the rain.*

My warmest thanks are to those who have true love for me and whose moral support and useful suggestions encouraged me at every step.

May Allah bless all those who pray for me (Ameen)

Maria Imtiaz

Preface

The study of boundary layer flows over stationary or moving surfaces has gained much interest in recent years due to its relevance in industrial and technological applications. For example heat treatment of material traveling between a feed roll and wind-up roll or a conveyer belts, melt spinning process in the extrusion of polymers continuous casting, glass blowing, cooling of a large metallic plate in a bath etc. Sakiadis [1] started the pioneering work on the boundary layer flows over continuously moving flat surfaces. This idea for stretching sheet was considered by Crane [2]. A closed form exact analytical solution has been provided in this study. Rajagopal et al. [3] performed an analytical investigation of viscoelastic boundary layer flow over a stretching sheet. Sankara and Watson [4] discussed the flow of micropolar fluid over a stretching sheet. Flow of an electrically conducting power-law fluid over a stretching sheet has been investigated by Andersson et al. [5]. Stagnation-point flow of second grade (viscoelastic) fluid over a stretching sheet was considered by Mahapatra and Gupta [6]. Numerical investigation of mass transfer in the two-dimensional flow of viscoelastic fluid has been conducted by Cortell [7]. Recently various investigations concerning the boundary layer flow analysis of viscous and non-Newtonian fluids have been reported (see Bachok et al. [8], Yacob et al. [9], Mustafa et al. [10], Hayat et al. [11]). The mentioned studies above are only confined to the boundary layer flows over a linearly stretching sheet. However it is evident that in industrial processes the sheet can be stretched in a variety of ways. In this regard, few attempts on the boundary layer flow over an exponentially stretching sheet have been reported. For instance Magyari and Keller [12] examined the characteristics of heat and mass transfer in the flow past an exponentially stretching surface. Flow and heat transfer over an exponentially stretching sheet with suction has been studied by Elbashbeshy [13]. Analytic solutions for flow of viscoelastic fluid over an exponentially stretching sheet have been provided by Khan and Sanjayanand [14]. Homotopy solutions for flow and heat transfer over an exponentially stretching sheet with thermal radiation are obtained by Sajid and Hayat [15].

Choi [16] experimentally verified that addition of small amount of nanoparticles appreciably increases the effective thermal conductivity of the base fluid. These particles

can be found in the metals such as (Al, Cu), oxides (Al_2O_3), carbides (SiC), nitrides (AlN, SiN) or nonmetals (Graphite, carbon nanotubes) contain these nanoparticles. Convective heat transfer in the flow of nanofluid past a flat plate has been studied by Kuznetsov and Nield [17]. The Cheng-Minkowcz problem for natural convective boundary layer flow in a porous medium filled with nanofluid taking into account the combined effects of Brownian motion and thermophoretic diffusion of nanoparticles has been analyzed by Nield and Kuznetsov [18]. Khan and Pop [19] have done the pioneering work on the boundary layer flow of nanofluid over a stretching sheet. Rana and Bhargava [20] extended this concept for a nonlinearly stretching sheet. Makinde and Aziz [21] numerically examined the flow of nanofluid over a linearly stretching sheet with convective boundary conditions. Nadeem and Lee [22] examined the boundary layer flow of nanofluid by stretched surface.

Motivated by the mentioned studies, we organized this dissertation as follows.

Chapter one includes some basic definitions and equations.

Chapter two addresses the Boundary layer flow of nanofluid over an exponentially stretching surface. Series solution of the developed problem is obtained by homotopic approach. Plots are prepared and analyzed.

Chapter three studies the boundary layer flow of an electrically conducting nanofluid past an exponentially stretching sheet in the presence of thermal radiation. Moreover the viscous dissipation effects are also accounted in the present flow configuration. The problem is first modeled and then solved analytically by applying homotopy analysis method [23-31]. The behaviors of Brownian motion and thermophoretic diffusion of nanoparticles have been examined graphically. The dimensionless expressions of reduced Nusselt number and reduced Sherwood number have been evaluated and discussed.

Contents

1	Fundamental laws	3
1.1	Newtonian fluids	3
1.2	Nonlinear fluids	4
1.3	Nanofluids	4
1.4	Dimensionless numbers	5
1.4.1	Brownian motion parameter	5
1.4.2	Thermophoresis parameter	5
1.4.3	Lewis number	5
1.4.4	Prandtl number	6
1.4.5	Eckert number	6
1.4.6	Hartman number	6
1.4.7	Reynolds number	7
1.5	Basic equations	7
1.5.1	Mathematical form of continuity equation	7
1.5.2	Mathematical form of linear Momentum	7
1.5.3	Law of conservation of energy	7
1.5.4	Law of conservation of concentration	10
1.6	Solution methodology	10
1.6.1	Homotopy	10
2	Flow of nanofluid on an exponentially stretching sheet	11
2.1	Mathematical development	11

2.2	Homotopy solution	13
2.2.1	Zeroth order deformation equations	14
2.2.2	Problems at mth-order deformation	15
2.3	Convergence of HAM solution	16
2.4	Discussion	19
2.5	Conclusions	29
3	MHD flow of nanofluid with viscous dissipation and radiation effects	30
3.1	Mathematical development	30
3.2	Homotopy solution	32
3.2.1	Zeroth order deformation equations	33
3.2.2	Problems at mth-order deformation	34
3.3	Convergence of HAM solution	36
3.4	Results and discussion	38
3.5	Concluding remarks	51

Chapter 1

Fundamental laws

In this chapter, we describe some basic definitions and fundamental laws related to fluid flow behavior. Also discussed solution methodology (Homotopy analysis method).

1.1 Newtonian fluids

Fluids obeying the viscosity expression by Newton are called the Newtonian fluids. These fluids are subjected to a linear connection between the shear rate and shear stress. In mathematical form we can write the Newton's law of viscosity as

$$\tau_{yx} \propto \frac{du}{dy}, \quad (1.1)$$

$$\tau_{yx} = \mu \frac{du}{dy}. \quad (1.2)$$

In above expression τ_{xy} is the shear stress, u is the velocity in the x -direction, du/dy is the shear rate and μ is the constant of proportionality which is called the absolute or dynamic viscosity. Infact dynamics of Newtonian fluids describes the flow phenomena of gases and of liquids containing small molecules (i.e., molecules with a molecular weight of less than about 1000). Examples of Newtonian fluid include water, sugar solutions, glycerin, light-hydrocarbon oils and silicone oils.

1.2 Nonlinear fluids

The fluids which do not satisfy the viscosity expression given by Newton. There is nonlinear relation between shear stress and shear rate for such fluids. Mathematically one can write

$$\tau_{yx} \propto \left(\frac{du}{dy} \right)^n, n \neq 1, \quad (1.3)$$

$$\tau_{yx} = k \left(\frac{du}{dy} \right)^n. \quad (1.4)$$

Here n denotes the flow behavior index and k the consistency index. Eq. (1.4) reduces to the Newton's law of viscosity when $n = 1$ and $k = \mu$. From Eq. (1.4) we have

$$\tau_{yx} = \eta \left(\frac{du}{dy} \right), \quad (1.5)$$

with the following definition of the apparent viscosity η is

$$\eta = k \left(\frac{du}{dy} \right)^{n-1}. \quad (1.6)$$

1.3 Nanofluids

These are the fluids which consist of nanometer-sized particles. The nanoparticles are typically made of metals, oxides, carbides or carbon nanotubes. Ordinary fluids include water, ethylene glycol and oil. Traditional fluid with nanoparticle enhances the heat transfer. Novel attributes of nanofluid made them capable to use in various applications, including engine cooling, domestic refrigerator, chiller, heat exchanger, nuclear reactor coolant and in boiler flue gas temperature reduction. Nanoparticles effect the heat and mass transfer characteristics. Thermal conductivity and convective heat transfer in nanofluids are greater when compared with the traditional fluid.

1.4 Dimensionless numbers

1.4.1 Brownian motion parameter

Brownian motion of nanoparticles is due to their random motion in base fluid which produces from collision of nanoparticles with base fluid. Such motion is because of size of the nanoparticles varying the heat transfer properties. In mathematical form we have

$$Br = \frac{\tau D_B (C_w - C_\infty)}{\nu}. \quad (1.7)$$

In above expression τ denotes the ratio of nanoparticles and fluid heat capacity respectively, D_B represents the Brownian diffusion coefficient, C_w and C_∞ the wall and fluid concentration and ν the kinematic viscosity.

1.4.2 Thermophoresis parameter

Such parameter is positive and negative for cold and hot surface respectively. For hot surface, thermophoresis moves the nanoparticle concentration boundary layer away from the wall. As a result, a particle-free layer is formed at the boundary and therefore the nanoparticle distribution is obtained just outside. In mathematical form one can write

$$Tr = \frac{\tau D_T (T_w - T_\infty)}{T_\infty \nu}, \quad (1.8)$$

In which D_T is thermophoretic diffusion coefficient and T_w and T_∞ denote respectively the wall and fluid temperatures.

1.4.3 Lewis number

It is defined as follows

$$\text{Lewis number } (L) = \frac{\text{Thermal diffusivity}}{\text{Mass diffusivity}} = \frac{\nu}{D_B}, \quad (1.9)$$

in which ν depicts the thermal diffusivity and D_B the mass diffusivity. Molecular diffusivity decreases when Lewis number is increased.

1.4.4 Prandtl number

A number which approximates the ratio of viscous diffusivity to thermal diffusivity. Mathematically one can write

$$\text{Pr} = \frac{\text{Viscous diffusivity}}{\text{Thermal diffusion rate}} = \frac{\nu}{\alpha} = \frac{\nu \rho c_p}{k}. \quad (1.10)$$

It should be pointed out that the heat diffuses very quickly relative to the velocity for small Pr. In Eq. (1.10), ν denotes the kinematic viscosity, c_p the specific heat and k the thermal conductivity.

1.4.5 Eckert number

It yields a ratio of a flow's kinetic energy and enthalpy. Dissipation is characterized by this number. We can express it mathematically as follows.

$$E = \frac{\text{Kinetic energy}}{\text{Enthalpy}} = \frac{u^2}{c_p (T_u - T_l)}, \quad (1.11)$$

where u is a characteristic flow velocity, c_p the constant-pressure specific heat of the flow and $(T_u - T_l)$ a characteristic temperature difference of the flow.

1.4.6 Hartman number

Ratio of magnetic body force and the viscous force is known as Hartman number i-e

$$Hr = \frac{\text{Magnetic forces}}{\text{viscous forces}} = \sqrt{\frac{B_0^2 d^2}{\mu_0 \rho \nu \lambda}}. \quad (1.12)$$

In Eq. (1.12) μ_0 represents the magnetic permeability and λ the magnetic diffusivity. Further B_0 represents characteristic magnetic field and d system length scale.

1.4.7 Reynolds number

It is characterized as ratio of inertial force and viscous force. It is mathematically represented by the following expression

$$\text{Reynolds number} = \frac{\text{Inertial force}}{\text{Viscous force}} = \frac{\rho \mathbf{V} L}{\mu} = \frac{\mathbf{V} L}{\nu}, \quad (1.13)$$

in which \mathbf{V} is the mean velocity of the object relative to the fluid, L denotes the characteristic length, μ the dynamic viscosity and ρ represents the fluid density.

1.5 Basic equations

1.5.1 Mathematical form of continuity equation

In view of no sources/sinks, one can write

$$\frac{\partial \rho}{\partial t} + \nabla \cdot (\rho \mathbf{V}) = 0, \quad (1.14)$$

where ρ signifies the density of fluid, t characterizes the time and \mathbf{V} denotes the velocity of fluid. The above equation for an incompressible fluid reduces to

$$\nabla \cdot \mathbf{V} = 0. \quad (1.15)$$

1.5.2 Mathematical form of linear Momentum

We have

$$\rho \frac{d\mathbf{V}}{dt} = -\nabla p + \mu \nabla^2 \mathbf{V}. \quad (1.16)$$

The above mathematical expression includes three forces namely the inertial, pressure and viscous.

1.5.3 Law of conservation of energy

The energy equation for nanofluid is

$$\rho c_p \frac{d\mathbf{T}}{dt} = -\text{div } \vec{q} + l_p \nabla \cdot \vec{\mathbf{j}}_p, \quad (1.17)$$

where c_p is specific heat of nanofluid, l_p is the specific enthalpy for nanoparticles, \vec{q} denotes the energy flux and $\vec{\mathbf{j}}_p$ the nanoparticles diffusion mass flux. Where energy flux \vec{q} is

$$\vec{q} = -k \nabla T + l_p \vec{\mathbf{j}}_p. \quad (1.18)$$

Substituting Eq.(1.17) into Eq. (1.18) we have

$$\begin{aligned} \rho c_p \frac{d\mathbf{T}}{dt} &= -\nabla \cdot (-k \nabla T + l_p \vec{\mathbf{j}}_p) + l_p \nabla \cdot \vec{\mathbf{j}}_p, \\ &= k \nabla^2 T - \nabla \cdot (l_p \vec{\mathbf{j}}_p) + l_p \nabla \cdot \vec{\mathbf{j}}_p, \\ &= k \nabla^2 T - l_p \nabla \cdot \vec{\mathbf{j}}_p - \vec{\mathbf{j}}_p \cdot \nabla l_p + l_p \nabla \cdot \vec{\mathbf{j}}_p, \\ &= k \nabla^2 T - \vec{\mathbf{j}}_p \cdot \nabla l_p. \end{aligned} \quad (1.19)$$

Using

$$\nabla l_p = c_p \nabla T, \quad (1.20)$$

one obtains from Eq. (1.19)

$$\rho c_p \frac{d\mathbf{T}}{dt} = k \nabla^2 T - c_p \vec{\mathbf{j}}_p \cdot \nabla T. \quad (1.21)$$

in which c_p is the nanoparticle specific heat of nanoparticles. Nanoparticles diffusion mass flux $\vec{\mathbf{j}}_p$ (the sum of Brownian and thermophoresis diffusion) is

$$\vec{\mathbf{j}}_p = \vec{\mathbf{j}}_{p,B} + \vec{\mathbf{j}}_{p,T}, \quad (1.22)$$

with

$$\vec{\mathbf{j}}_{p,B} = -\rho_p D_B \nabla C, \quad (1.23)$$

where the Brownian diffusion coefficient D_B in view of Einstein–Stokes equation is

$$D_B = \frac{k_B T}{3\pi\mu d_p}, \quad (1.24)$$

where k_B represents the Boltzmann's constant and d_p the diameter of nanoparticles.

$$\vec{\mathbf{j}}_{p,T} = \rho_p C \vec{V}_\tau, \quad (1.25)$$

$$\vec{V}_\tau = -\tilde{\beta} \frac{\mu}{\rho} \frac{\nabla T}{T}, \quad (1.26)$$

in which \vec{V}_τ represents the thermophoretic velocity and $\tilde{\beta}$ the proportionality factor given by

$$\tilde{\beta} = 0.26 \frac{k}{2k + k_p}, \quad (1.27)$$

where k and k_p are the fluid and the particle material thermal conductivities respectively. The thermophoresis diffusion flux can be expressed as follows.

$$\vec{\mathbf{j}}_{p,T} = -\rho_p D_T \frac{\nabla T}{T}, \quad (1.28)$$

with

$$D_T = \frac{\tilde{\beta} \mu C}{\rho}, \quad (1.29)$$

as the thermophoretic diffusion coefficient. Diffusion mass flux through Eqs. (1.23) and (1.27) is

$$\vec{\mathbf{j}}_p = -\rho_p D_B \nabla C - \rho_p D_T \frac{\nabla T}{T}, \quad (1.30)$$

and thus Eq. (1.21) becomes

$$\rho c_p \frac{d\mathbf{T}}{dt} = k \nabla^2 T + \rho_p c_p \left[D_B \nabla C \cdot \nabla T + \rho_p D_T \frac{\nabla T \cdot \nabla T}{T} \right]. \quad (1.31)$$

1.5.4 Law of conservation of concentration

The nanoparticles concentration equation is

$$\frac{\partial C}{\partial t} + \vec{\mathbf{V}} \cdot \nabla C = -\frac{1}{\rho_p} \nabla \cdot \vec{\mathbf{j}}_p, \quad (1.32)$$

in which C denotes the concentration, ρ_p the mass density and $\vec{\mathbf{j}}_p$ the diffusion mass flux. Making use of Eq. (1.30) into Eq. (1.32) we have

$$\frac{\partial C}{\partial t} + \vec{\mathbf{V}} \cdot \nabla C = \nabla \cdot \left[D_B \nabla C + D_T \frac{\nabla T}{T} \right]. \quad (1.33)$$

1.6 Solution methodology

Physical problem in fluid mechanics are always nonlinear. Exact solutions to such problems are not easy to find. Hence the researchers then rely on the numerical and approximate solutions. Amongst the various techniques there is one called homotopy analysis method. Series solution is developed in this method.

1.6.1 Homotopy

Two functions are called homotopic if one function can be deformed continuously into the other function. Two continuous maps (m_1 and m_2) from the topological space A into the topological space B are called homotopic if there exists a continuous map M

$$M : A \times [0, 1] \rightarrow B$$

such that for each $a \in A$

$$M(a, 0) = m_1(a), \quad M(a, 1) = m_2(a)$$

The map M is called the homotopy between m_1 and m_2 .

Chapter 2

Flow of nanofluid on an exponentially stretching sheet

Let us investigate the flow of viscous nanofluid on an exponentially stretching surface. Series solutions to the developed equations are obtained. Plots of velocity, temperature and nanoparticle concentration are given and discussed for suction/injection parameter λ , Prandtl number Pr , Lewis number L , Brownian motion parameter Br and thermophoresis parameter Tr . Interpretation to various physical quantities of interest is made. The contents of this chapter provides a review of a paper by Nadeem and Lee [22].

2.1 Mathematical development

We study the incompressible nanofluid flow induced by an exponentially stretching sheet. Sheet possess stretching property along x -axis with velocity $U_w = U_0 e^{\frac{x}{l}}$ at $y = 0$ and y -axis is normal to it. The equations which govern the present flow situation are

$$\frac{\partial u}{\partial x} + \frac{\partial v}{\partial y} = 0, \quad (2.1)$$

$$u \frac{\partial u}{\partial x} + v \frac{\partial u}{\partial y} = \nu \frac{\partial^2 u}{\partial y^2}, \quad (2.2)$$

$$u \frac{\partial T}{\partial x} + v \frac{\partial T}{\partial y} = \alpha \frac{\partial^2 T}{\partial y^2} + \frac{(\rho c)_p}{(\rho c)_f} \left[D_B \frac{\partial C}{\partial y} \frac{\partial T}{\partial y} + \frac{D_T}{T_\infty} \left(\frac{\partial T}{\partial y} \right)^2 \right], \quad (2.3)$$

$$u \frac{\partial C}{\partial x} + v \frac{\partial C}{\partial y} = D_B \frac{\partial^2 C}{\partial y^2} + \frac{D_T}{T_\infty} \frac{\partial^2 T}{\partial y^2}. \quad (2.4)$$

In above equations ρ_f represents the base fluid density, T denotes temperature, C the nanoparticle concentration, $(\rho c)_p$ shows the nanoparticles heat capacity, $(\rho c)_f$ the fluid heat capacity, $\alpha = k/(\rho c)_f$ depicts the fluid thermal diffusivity, D_B denotes the Brownian diffusion coefficient and D_T represents the thermophoretic diffusion coefficient.

The subjected conditions are mentioned below.

$$\begin{aligned} u &= U_w(x) = U_0 e^{\frac{x}{l}}, \quad v = -\beta(x), \quad T = T_w, \quad C = C_w \quad \text{at } y = 0, \\ u &= 0, \quad T = T_\infty, \quad C = C_\infty \quad \text{as } y \rightarrow \infty, \end{aligned} \quad (2.5)$$

where U_0 denotes reference velocity, $\beta(x)$ the suction and injection velocity with $\beta(x) > 0$ and $\beta(x) < 0$ respectively, T_w and T_∞ are the respective wall temperature and temperature far away from the surface, C_w and C_∞ are the concentration of wall and ambient fluid.

Using

$$\begin{aligned} \zeta &= y \sqrt{\frac{U_0}{2\nu l}} e^{\frac{x}{2l}}, \quad u = U_0 e^{\frac{x}{l}} F'(\zeta), \quad v = -\sqrt{\frac{\nu U_0}{2l}} e^{\frac{x}{2l}} [F(\zeta) + \zeta F'(\zeta)], \\ G(\zeta) &= \frac{T - T_\infty}{T_w - T_\infty}, \quad J(\zeta) = \frac{C - C_\infty}{C_w - C_\infty}. \end{aligned} \quad (2.6)$$

Eq. (2.1) is satisfied automatically and Eqs. (2.2) – (2.4) are reduced as follows.

$$F''' - 2F'^2 + FF'' = 0, \quad (2.7)$$

$$\frac{1}{\text{Pr}} G'' + FG' + BrG'J' + TrG'^2 = 0, \quad (2.8)$$

$$J'' + LFJ' + \frac{Tr}{Br} G'' = 0, \quad (2.9)$$

$$\begin{aligned} F(0) &= -\lambda, \quad F'(0) = 1, \quad G(0) = 1, \quad J(0) = 1, \\ F'(\infty) &= 0, \quad G(\infty) = 0, \quad J(\infty) = 0, \end{aligned} \quad (2.10)$$

where the Prandtl number Pr , Lewis number L , Brownian motion parameter Br and thermophoresis parameter Tr are

$$Pr = \frac{\nu}{\alpha}, \quad L = \frac{\nu}{D_B}, \quad Br = \frac{(\rho c)_p D_B (C_w - C_\infty)}{(\rho c)_f \nu}, \quad Tr = \frac{(\rho c)_p D_T (T_w - T_\infty)}{(\rho c)_f T_\infty \nu}. \quad (2.11)$$

Local skin-friction C_f , Nusselt number Nu and the Sherwood number Sh are given as

$$C_f = \frac{\tau_w|_{y=0}}{\frac{1}{2}\rho U_0^2 e^{\frac{2x}{l}}}, \quad Nu = -\frac{x}{(T_w - T_\infty)} \frac{\partial T}{\partial y} \Big|_{y=0}, \quad Sh = -\frac{x}{(C_w - C_\infty)} \frac{\partial C}{\partial y} \Big|_{y=0}, \quad (2.12)$$

$$C_f \sqrt{\frac{Re_x}{2}} = F''(0), \quad Nu Re_x^{-1/2} \sqrt{\frac{2l}{x}} = -G'(0), \quad Sh Re_x^{-1/2} \sqrt{\frac{2l}{x}} = -J'(0), \quad (2.13)$$

in which $Re_x = U_0 e^{\frac{x}{l}} x / \nu$ denotes the local Reynolds number.

2.2 Homotopy solution

Initial guess and the linear operators $\mathcal{L}_n (n = 1 - 3)$ are chosen as

$$F_0(\varsigma) = 1 - S - e^{-\varsigma}, \quad G_0(\varsigma) = e^{-\varsigma}, \quad J_0(\varsigma) = e^{-\varsigma}, \quad (2.14)$$

$$\mathcal{L}_F = F''' - F', \quad \mathcal{L}_G = G'' - G, \quad \mathcal{L}_J = J'' - J. \quad (2.15)$$

The above operators satisfy the following expressions

$$\mathcal{L}_F(A_1 + A_2 e^\varsigma + A_3 e^{-\varsigma}) = 0, \quad (2.16)$$

$$\mathcal{L}_G(A_4 e^\varsigma + A_5 e^{-\varsigma}) = 0, \quad (2.17)$$

$$\mathcal{L}_J(A_6 e^\varsigma + A_7 e^{-\varsigma}) = 0, \quad (2.18)$$

where $A_n (n = 1 - 7)$ are the arbitrary constants.

2.2.1 Zeroth order deformation equations

The zeroth-order deformation problems through Eq. (2.7) – (2.9) can be constructed as follows:

$$(1 - w) \mathcal{L}_F \left[\widehat{F}(\varsigma; w) - F_0(\varsigma) \right] = w \hbar_F \mathcal{N}_F \left[\widehat{F}(\varsigma; w) \right], \quad (2.19)$$

$$\widehat{F}(0; w) = -S, \quad \widehat{F}'(0; w) = 1, \quad \widehat{F}'(\infty; w) = 0, \quad (2.20)$$

$$(1 - w) \mathcal{L}_G \left[\widehat{G}(\varsigma; w) - G_0(\varsigma) \right] = w \hbar_G \mathcal{N}_G \left[\widehat{G}(\varsigma; w) \right], \quad (2.21)$$

$$\widehat{G}(0; w) = 1, \quad \widehat{G}(\infty; w) = 0, \quad (2.22)$$

$$(1 - w) \mathcal{L}_J \left[\widehat{J}(\varsigma; w) - J_0(\varsigma) \right] = w \hbar_J \mathcal{N}_J \left[\widehat{J}(\varsigma; w) \right], \quad (2.23)$$

$$\widehat{J}(0; w) = 1, \quad \widehat{J}(\infty; w) = 0, \quad (2.24)$$

In Eqs. (2.19) – (2.24), \hbar_F , \hbar_G & \hbar_J are the non-zero convergence control parameters, and the nonlinear operators $\mathcal{N}_F \left[\widehat{F}(\varsigma; w) \right]$, $\mathcal{N}_G \left[\widehat{G}(\varsigma; w) \right]$ and $\mathcal{N}_J \left[\widehat{J}(\varsigma; w) \right]$ of Eqs. (2.7) – (2.9) are given by

$$\mathcal{N}_F \left[\widehat{F}(\varsigma; w) \right] = \frac{\partial^3 \widehat{F}(\varsigma; w)}{\partial \varsigma^3} - 2 \left(\frac{\partial \widehat{F}(\varsigma; w)}{\partial \varsigma} \right)^2 + \widehat{F}(\varsigma; w) \frac{\partial^2 \widehat{F}(\varsigma; w)}{\partial \varsigma^2}, \quad (2.25)$$

$$\begin{aligned} \mathcal{N}_G \left[\widehat{G}(\varsigma; w) \right] &= \frac{1}{Pr} \frac{\partial^2 \widehat{G}(\varsigma; w)}{\partial \varsigma^2} + \widehat{F}(\varsigma; w) \frac{\partial \widehat{G}(\varsigma; w)}{\partial \varsigma} + Br \frac{\partial \widehat{G}(\varsigma; w)}{\partial \varsigma} \frac{\partial \widehat{J}(\varsigma; w)}{\partial \varsigma} \\ &+ Tr \left(\frac{\partial \widehat{G}(\varsigma; w)}{\partial \varsigma} \right)^2, \end{aligned} \quad (2.26)$$

$$\mathcal{N}_J \left[\widehat{J}(\varsigma; w) \right] = \frac{\partial^2 \widehat{J}(\varsigma; w)}{\partial \varsigma^2} + L \widehat{F}(\varsigma; w) \frac{\partial \widehat{J}(\varsigma; w)}{\partial \varsigma} + \frac{Tr}{Br} \frac{\partial^2 \widehat{G}(\varsigma; w)}{\partial \varsigma^2}, \quad (2.27)$$

When w changes from 0 to 1, then $\widehat{F}(\varsigma, w)$, $\widehat{G}(\varsigma, w)$ and $\widehat{J}(\varsigma, w)$ change from initial guesses $F_0(\varsigma)$, $G_0(\varsigma)$ and $J_0(\varsigma)$ to the final solutions $F(\varsigma)$, $G(\varsigma)$ and $J(\varsigma)$, respectively. Thus

$$\widehat{F}(\varsigma, 0) = F_0(\varsigma), \quad \widehat{F}(\varsigma, 1) = F(\varsigma), \quad (2.28)$$

$$\widehat{G}(\varsigma, 0) = G_0(\varsigma), \quad \widehat{G}(\varsigma, 1) = G(\varsigma), \quad (2.29)$$

$$\widehat{J}(\varsigma, 0) = J_0(\varsigma), \quad \widehat{J}(\varsigma, 1) = J(\varsigma). \quad (2.30)$$

Expanding $\widehat{F}(\varsigma, w)$, $\widehat{G}(\varsigma, w)$ and $\widehat{J}(\varsigma, w)$ in power series of the embedding parameter w as

$$\widehat{F}(\varsigma, w) = F_0(\varsigma) + \sum_{m=1}^{\infty} F_m(\varsigma)w^m; \quad F_m(\varsigma) = \left. \frac{1}{m!} \frac{\partial^m \widehat{F}(\varsigma, w)}{\partial w^m} \right|_{w=0}, \quad (2.31)$$

$$\widehat{G}(\varsigma, w) = G_0(\varsigma) + \sum_{m=1}^{\infty} G_m(\varsigma)w^m; \quad G_m(\varsigma) = \left. \frac{1}{m!} \frac{\partial^m \widehat{G}(\varsigma, w)}{\partial w^m} \right|_{w=0}, \quad (2.32)$$

$$\widehat{J}(\varsigma, w) = J_0(\varsigma) + \sum_{m=1}^{\infty} J_m(\varsigma)w^m; \quad J_m(\varsigma) = \left. \frac{1}{m!} \frac{\partial^m \widehat{J}(\varsigma, w)}{\partial w^m} \right|_{w=0}. \quad (2.33)$$

We select the parameters \hbar_F , \hbar_G and \hbar_J such that the Taylor series expansion of $\widehat{F}(\varsigma, w)$, $\widehat{G}(\varsigma, w)$ and $\widehat{J}(\varsigma, w)$ converge at $w = 1$ then by Eqs. (2.28) – (2.30), we get

$$F(\varsigma) = F_0(\varsigma) + \sum_{m=1}^{\infty} F_m(\varsigma), \quad (2.34)$$

$$G(\varsigma) = G_0(\varsigma) + \sum_{m=1}^{\infty} G_m(\varsigma), \quad (2.35)$$

$$J(\varsigma) = J_0(\varsigma) + \sum_{m=1}^{\infty} J_m(\varsigma). \quad (2.36)$$

2.2.2 Problems at m th-order deformation

Taking the derivative of zeroth order deformation Eqs. (2.19) – (2.24) m -times with respect to w and then setting $w = 0$, one has

$$\mathcal{L}_F [F_m(\varsigma) - \chi_m F_{m-1}(\varsigma)] = \hbar_F \mathcal{R}_m^F(\varsigma), \quad (2.37)$$

$$F_m(0) = F_m'(0) = F_m'(\infty) = 0, \quad (2.38)$$

$$\mathcal{L}_G [G_m(\varsigma) - \chi_m G_{m-1}(\varsigma)] = \hbar_G \mathcal{R}_m^G(\varsigma), \quad (2.39)$$

$$G_m(0) = G_m(\infty) = 0, \quad (2.40)$$

$$\mathcal{L}_J [J_m(\varsigma) - \chi_m J_{m-1}(\varsigma)] = \hbar_J \mathcal{R}_m^J(\varsigma), \quad (2.41)$$

$$J_m(0) = J_m(\infty) = 0, \quad (2.42)$$

$$\mathcal{R}_m^F(\varsigma) = \left[F_{m-1}''' - 2 \sum_{i=0}^{m-1} F_{m-1-i}' F_i' + \sum_{i=0}^{m-1} F_{m-1-i} F_i'' \right], \quad (2.43)$$

$$\mathcal{R}_m^G(\varsigma) = \frac{1}{Pr} G_{m-1}'' + \sum_{i=0}^{m-1} [F_{m-1-i} G_i' + Br G_{m-1-i}' J_i' + Tr G_{m-1-i}' G_i'], \quad (2.44)$$

$$\mathcal{R}_m^J(\varsigma) = \left[J_{m-1}'' + L \sum_{i=0}^{m-1} F_{m-1-i} J_i' + \frac{Tr}{Br} G_{m-1}'' \right], \quad (2.45)$$

$$\chi_m = \begin{cases} 0, & m \leq 1 \\ 1, & m > 1 \end{cases}. \quad (2.46)$$

The general solutions can be written as

$$F_m(\varsigma) = F_m^*(\varsigma) + A_1 + A_2 e^\varsigma + A_3 e^{-\varsigma}, \quad (2.47)$$

$$G_m(\varsigma) = G_m^*(\varsigma) + A_4 e^\varsigma + A_5 e^{-\varsigma}, \quad (2.48)$$

$$J_m(\varsigma) = J_m^*(\varsigma) + A_6 e^\varsigma + A_7 e^{-\varsigma}, \quad (2.49)$$

with F_m^* , G_m^* and J_m^* as the particular solutions and the constants A_n ($n = 1 - 7$) after using the boundary conditions (2.38), (2.40) and (2.42) are

$$\begin{aligned} A_1 &= -F_m^*(0) - A_3, \quad A_2 = A_4 = A_6 = 0, \quad A_3 = \left. \frac{\partial F_m^*(\varsigma)}{\partial \varsigma} \right|_{\varsigma=0}, \\ A_5 &= -G_m^*(0), \quad A_7 = -J_m^*(0). \end{aligned} \quad (2.50)$$

2.3 Convergence of HAM solution

Now the solution of Eqs. (2.7) – (2.9) along with the boundary conditions (2.10) is computed using homotopy analysis method. The values of non-zero auxiliary parameters \hbar_F , \hbar_G and \hbar_J have a key role in the convergence of series expressions. The \hbar -curves are plotted in the Figs. (2.1, 2.2 and 2.3) for velocity, temperature and concentration profiles. We have plotted the convergence region of velocity, temperature and concentration for various

values of suction/injection parameter λ . The range for admissible values of auxiliary parameters for $\lambda = 0.2$ are $-1.25 \leq \hbar_F \leq -0.25$, $-1.3 \leq \hbar_G \leq -0.6$, $-1.25 \leq \hbar_J \leq -0.55$, for $\lambda = 0.5$ are $-1.2 \leq \hbar_F \leq -0.2$, $-1.2 \leq \hbar_G \leq -0.5$, $-1.45 \leq \hbar_J \leq -0.5$ and for $\lambda = 1$ are $-1.15 \leq \hbar_F \leq -0.2$, $-1.25 \leq \hbar_G \leq -0.55$, $-1.2 \leq \hbar_J \leq -0.6$.

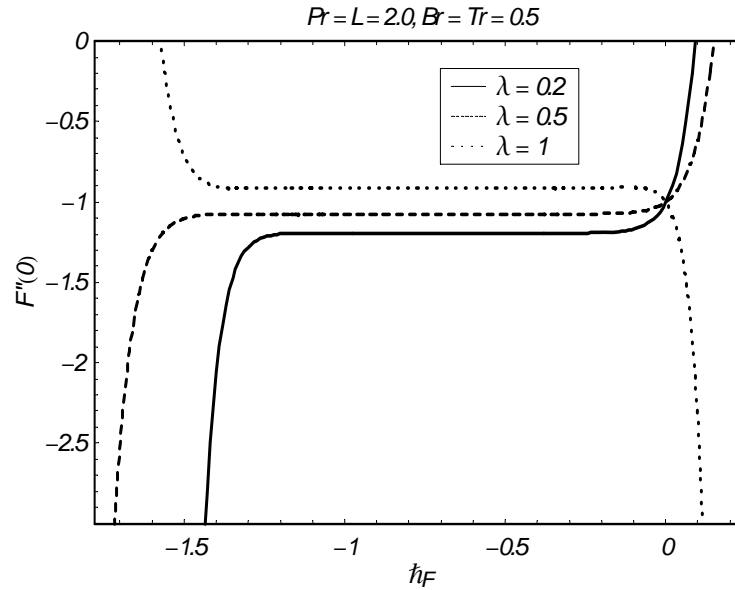


Fig. 2.1: \hbar -curves for velocity F .

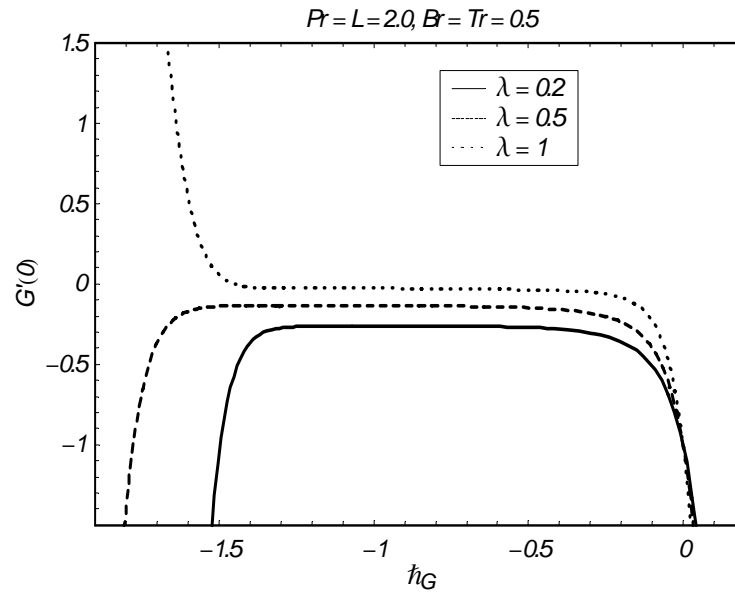


Fig. 2.2: \hbar -curves for temperature profile G .

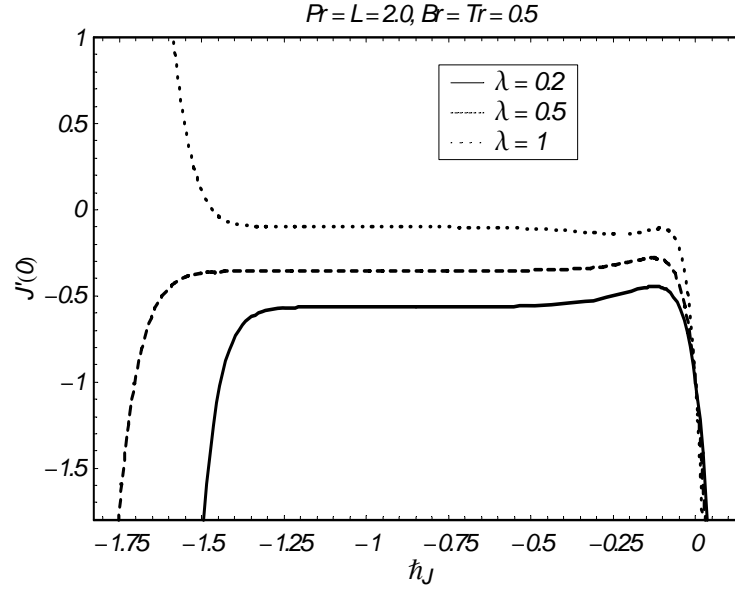


Fig. 2.3: h -curves for concentration profile J .

Table 2.1. Convergence of HAM solutions through different order of approximations when $Pr = 2.0 = L$, $\lambda = 0.2$, $Br = 0.5$ and $Tr = 0.5$.

Order of approximations	$-F''(0)$	$-G'(0)$	$-J'(0)$
1	1.18667	0.586667	0.306667
5	1.19315	0.312312	0.509637
10	1.19300	0.268941	0.558798
15	1.19299	0.263518	0.564679
20	1.19298	0.262803	0.565410
25	1.19298	0.262687	0.565497
30	1.19298	0.262666	0.565501
35	1.19298	0.262662	0.565502
40	1.19298	0.262661	0.565504
46	1.19298	0.262661	0.565504
50	1.19298	0.262661	0.565504
60	1.19298	0.262661	0.565504

2.4 Discussion

The velocity F' for different values of suction injection parameter λ against ζ is shown in Fig. 2.4. It is observed that velocity profile and boundary layer increase when λ increases. The temperature profile G for Prandtl number Pr , Brownian motion parameter Br , thermophoresis parameter Tr and Lewis number L is shown in the Figs. (2.5) – (2.8). In Fig. 2.5, effect of Pr on temperature profile is shown. When Pr increases, the temperature profile decreases. The variation of Br on G is shown in Fig. 2.6. By increasing Br , the temperature profile increases. Influence of Tr on G is depicted in Fig. 2.7. We observe that temperature profile and thermal boundary layer thickness increase when Tr is increased. There is a decrease in G by increasing L (Fig. 2.8). The nanoparticle concentration J for various values of Pr , Br , Tr and L is plotted in the Figs. (2.9) – (2.12). Effects of Pr on J are shown in Fig. 2.9. It is depicted that concentration profile increases when there is an increase in Pr . It is observed from Fig. 2.10 that when Br increases, J and boundary layer decreases. However J and thermal boundary layer thickness increase when Tr is increased (Fig. 2.11). Also J and thermal boundary layer thickness decrease by increasing L (Fig. 2.12).

Figs. (2.13) – (2.16) show the change in dimensionless heat and mass transfer rates versus Tr . It is noted from Fig. 2.13 and 2.14, that the dimensionless heat transfer rate decreases when there is an increase in Pr and L . Effects of Pr and L on the dimensionless concentration rates are displayed in the Figs. 2.15 and 2.16. It is observed from these Figs. that the dimensionless concentration rates increase when Pr and L are increased.

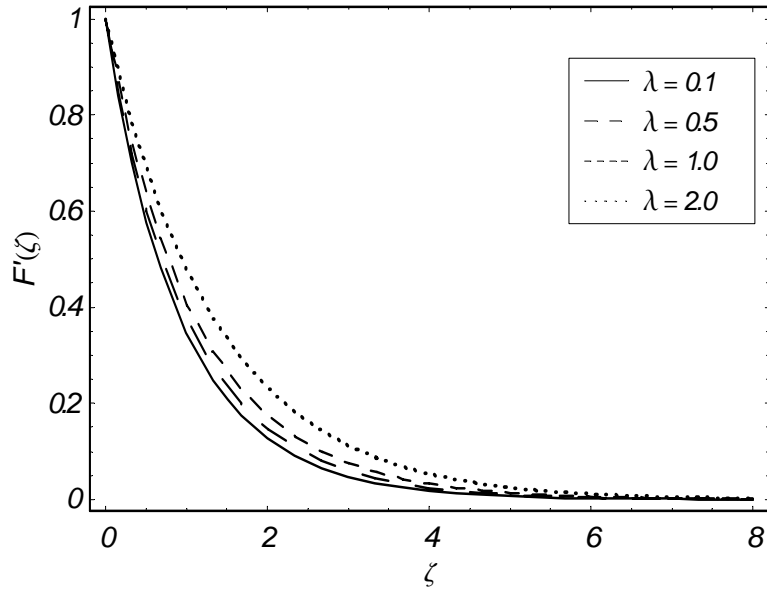


Fig. 2.4: Velocity for different values of λ .

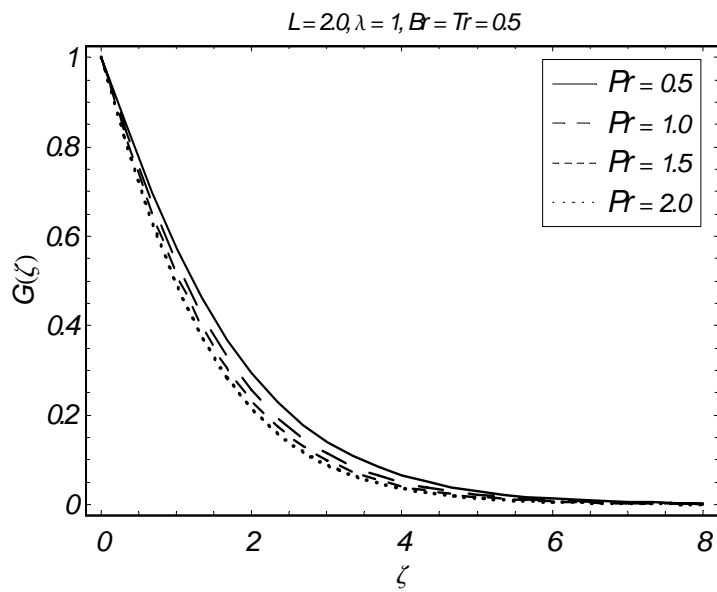


Fig. 2.5: Influence of Pr on G .

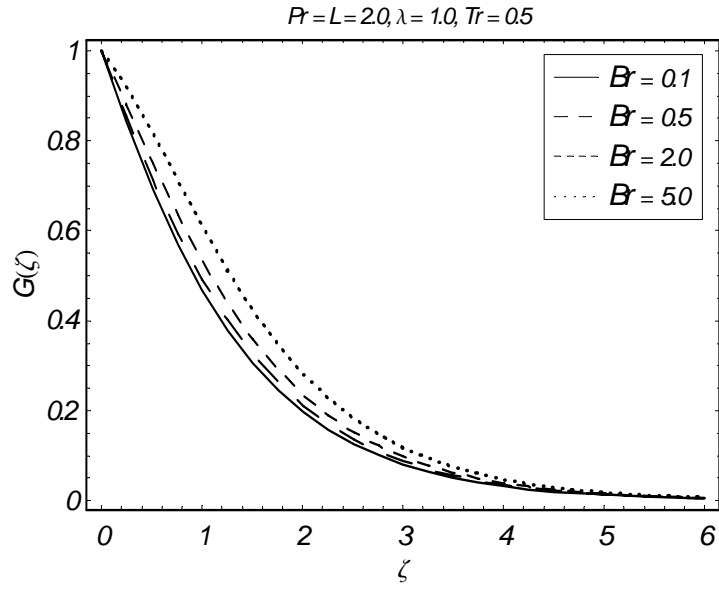


Fig. 2.6: Influence of Br on G .

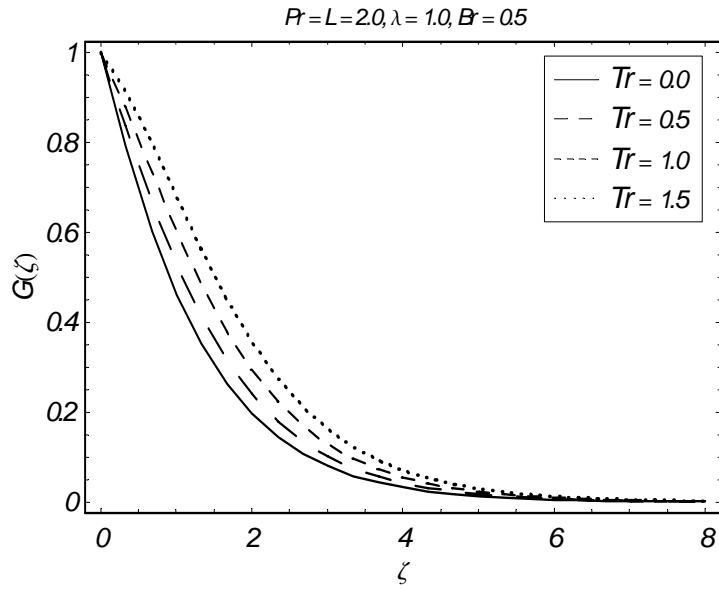


Fig. 2.7: Influence of Tr on G .

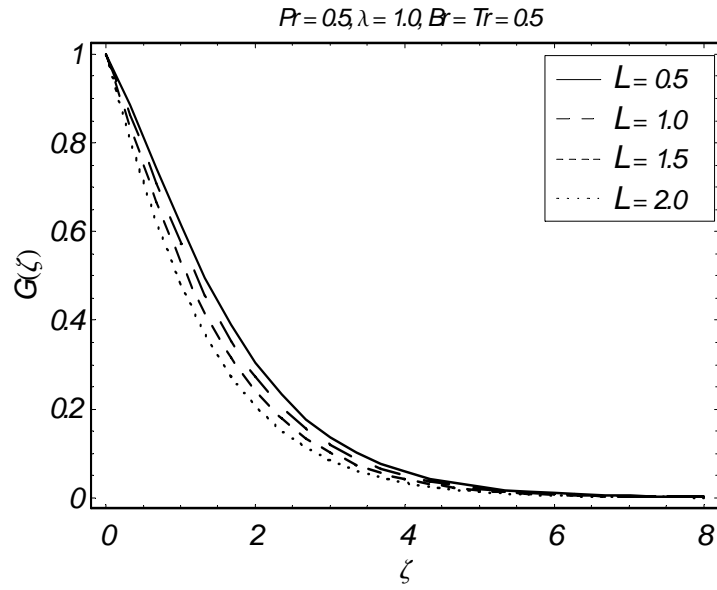


Fig. 2.8: Influence of L on G .

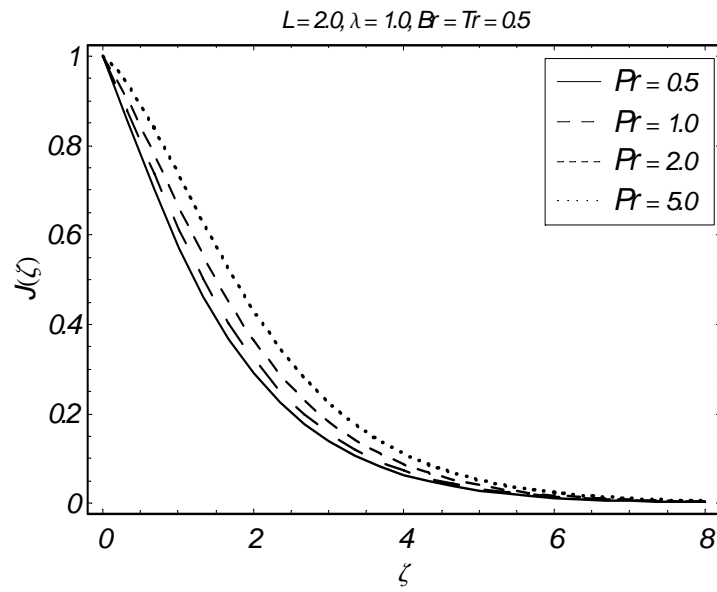


Fig. 2.9: Influence of Pr on J .

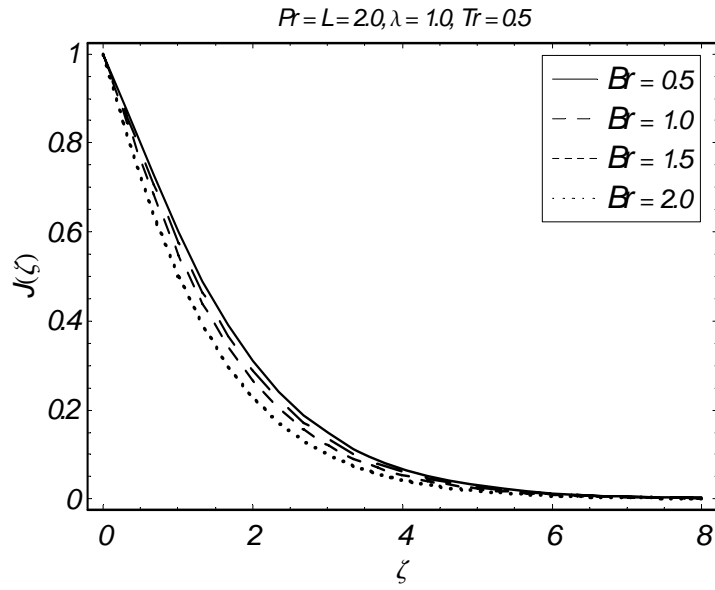


Fig. 2.10: Influence of Br on J .

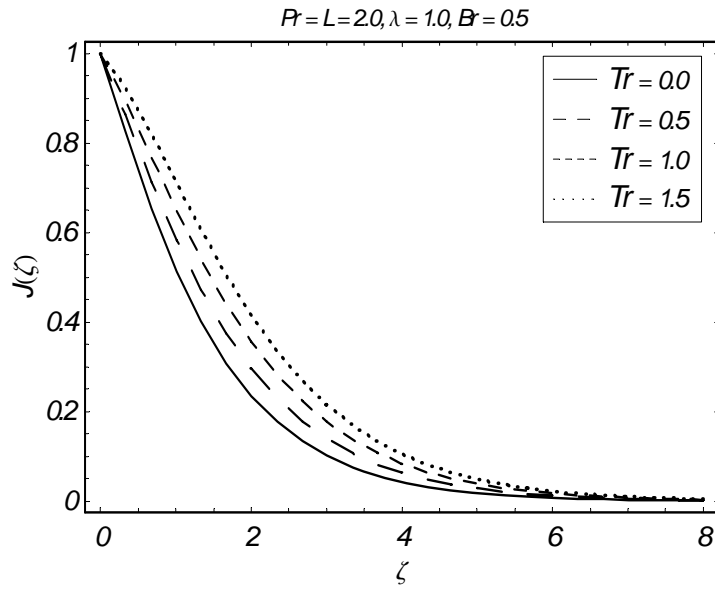


Fig. 2.11: Influence of Tr on J .

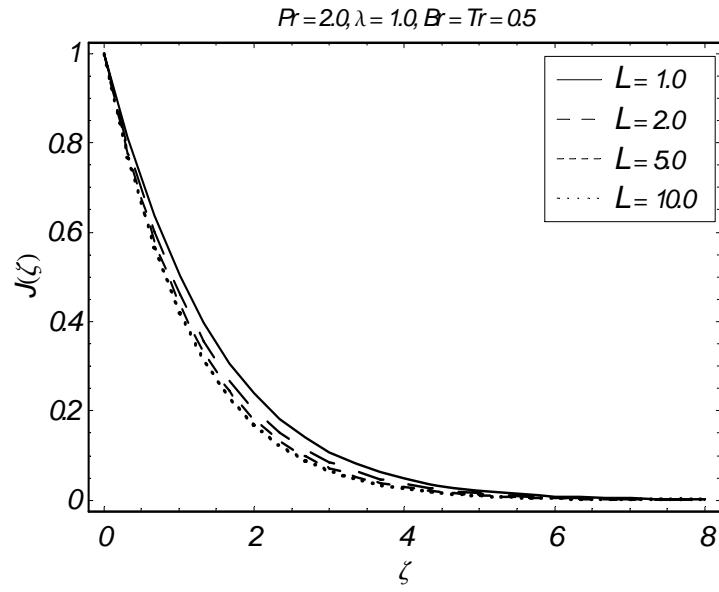


Fig. 2.12: Influence of L on J .

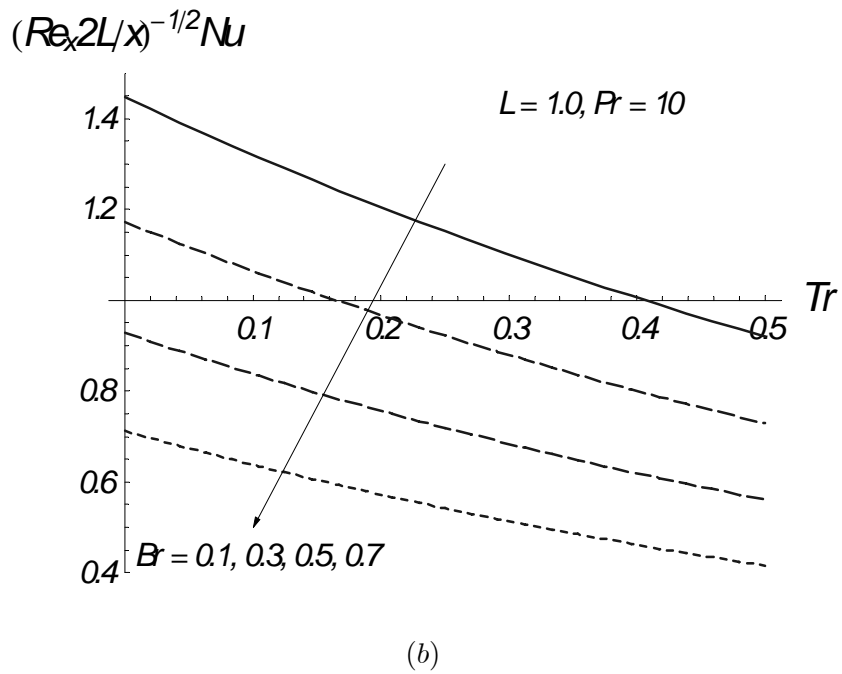
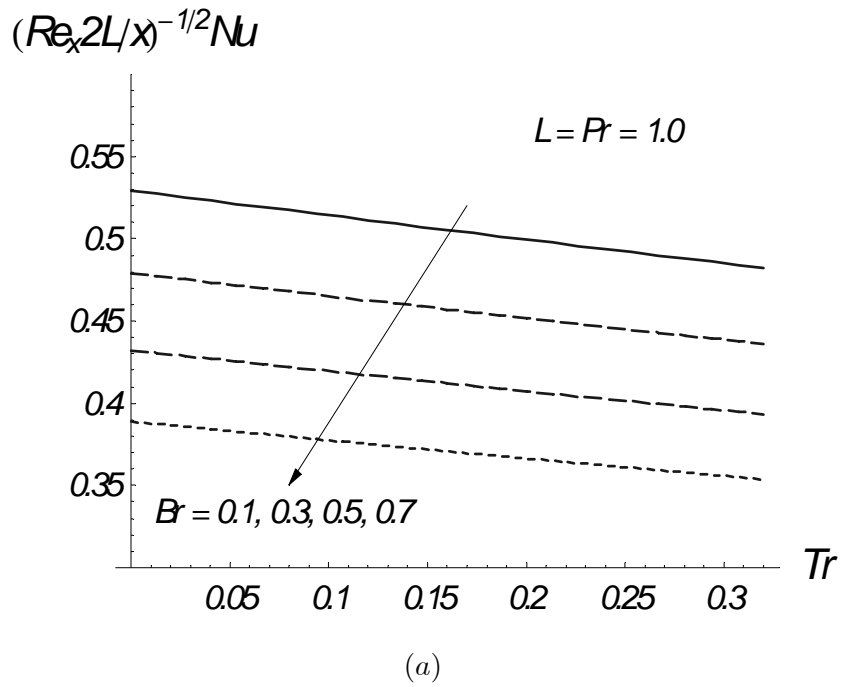
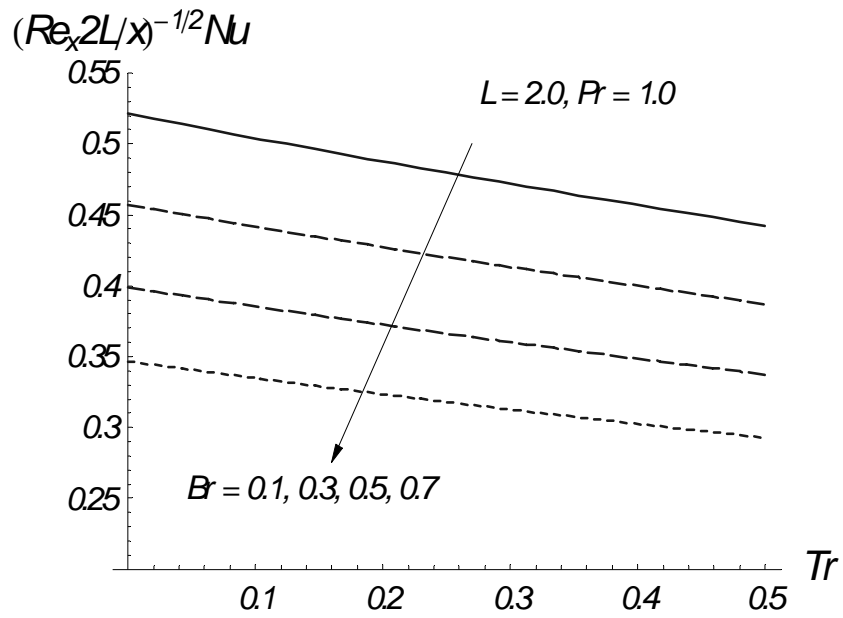
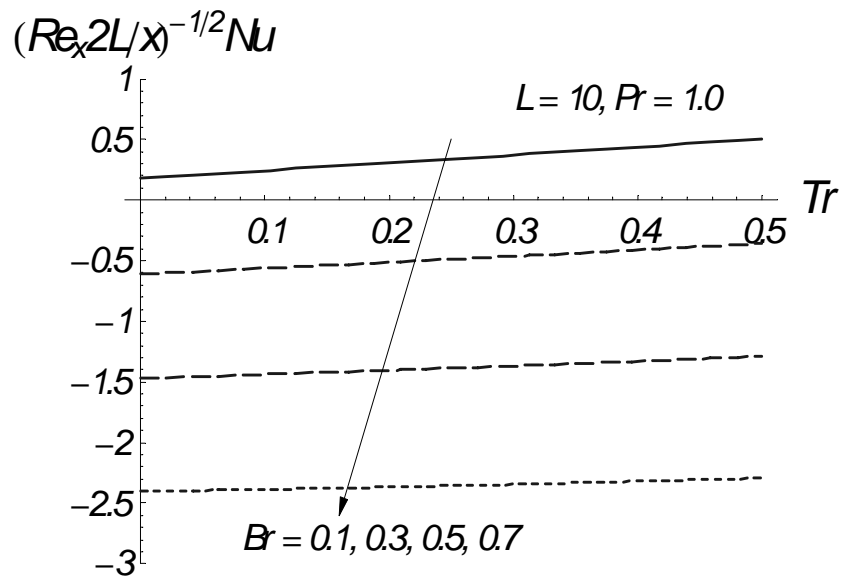


Fig. 2.13: Effects of Br and Pr on dimensionless heat transfer rates.



(a)



(b)

Fig. 2.14: Effects of Br and L on dimensionless heat transfer rates.

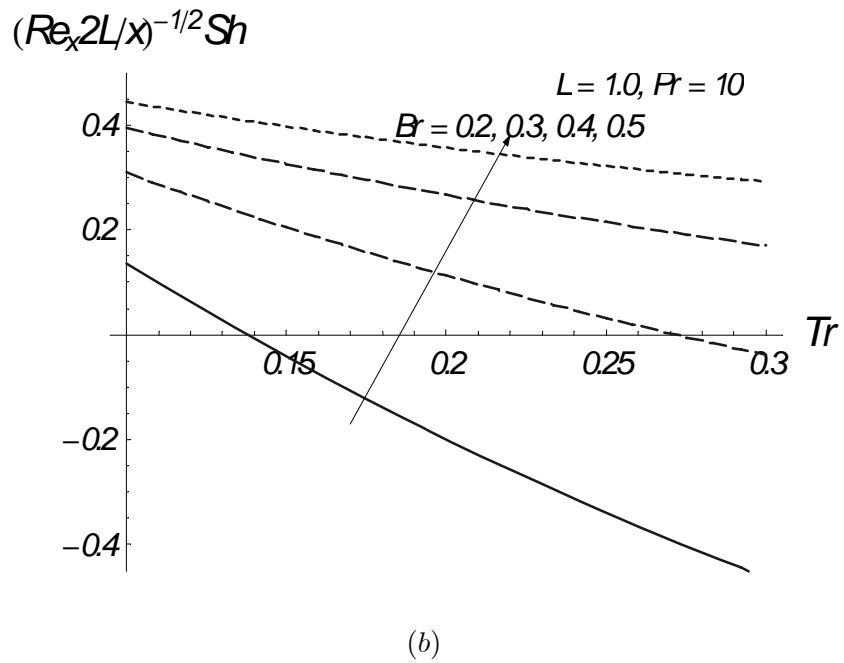
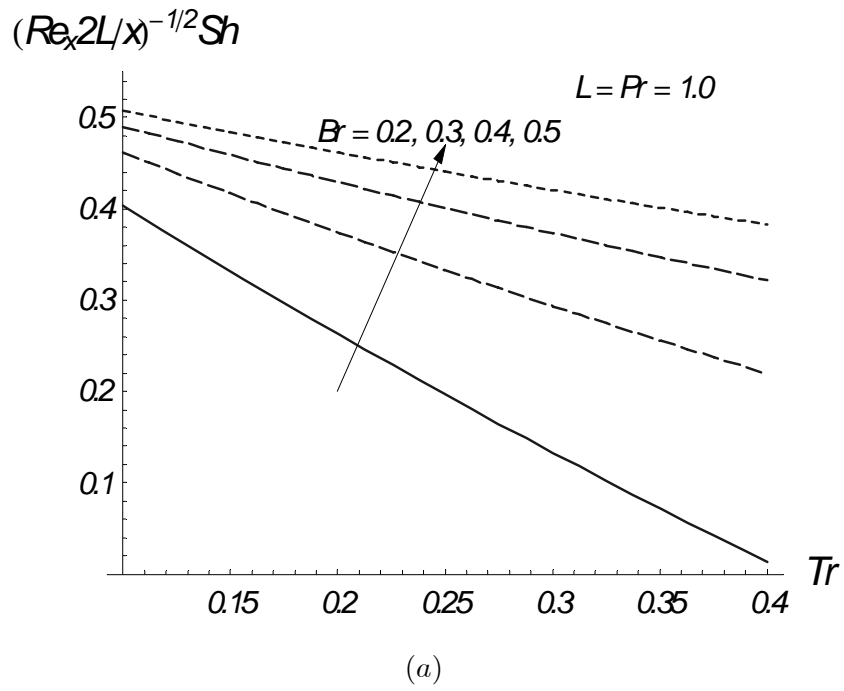
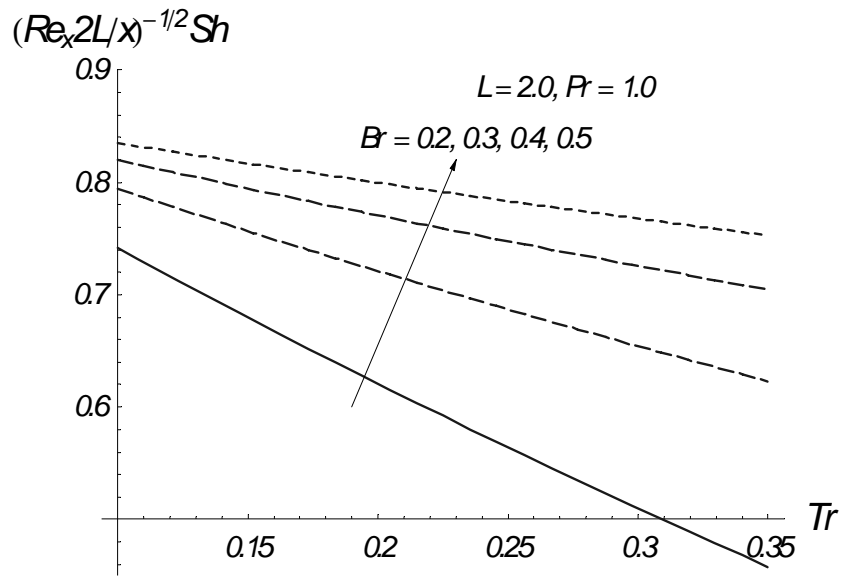
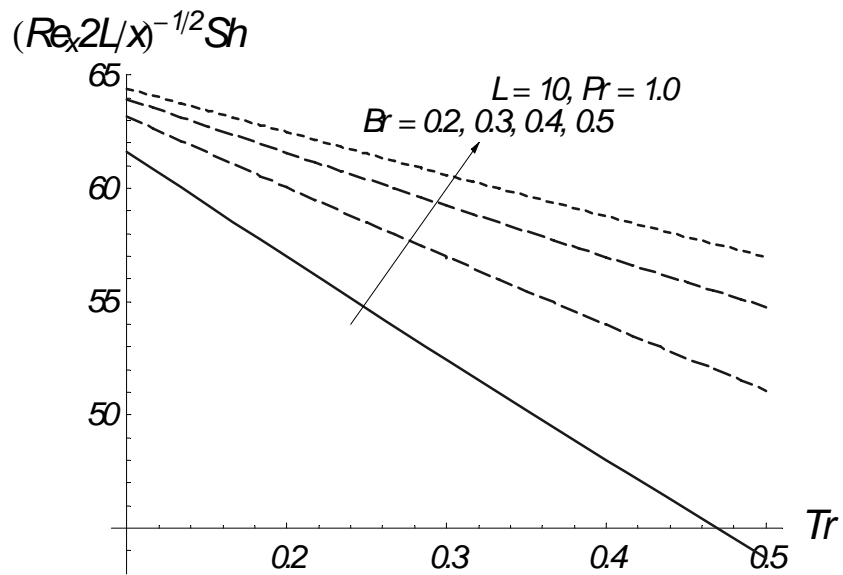


Fig. 2.15: Effects of Br and Pr on dimensionless concentration rates.



(a)



(b)

Fig. 2.16: Effects of Br and L on dimensionless concentration rates.

2.5 Conclusions

Nanofluid flow on an exponential stretching surface with suction and injection is discussed. The main points can be listed as follows.

- The temperature profile G decreases by increasing Prandtl number Pr and Lewis number L .
- Temperature profile increases by increasing Brownian motion parameter Br and thermophoresis parameter Tr .
- An increase in Prandtl number Pr and thermophoresis parameter Tr increases the concentration profile J .
- Effects of Brownian motion parameter Br and Lewis number L on the concentration profile are quite opposite to that of Pr and Tr .
- Reduced Nusselt number is a decreasing function of Br , Pr and L while the reduced Sherwood number is an increasing function of these parameters.

Chapter 3

MHD flow of nanofluid with viscous dissipation and radiation effects

This study looks at the effects of magnetohydrodynamics (MHD), thermal radiation and viscous dissipation in the flow analysis of previous chapter. The model used for the nanoparticle includes the effects of Brownian motion and thermophoresis. Homotopy analysis method is applied to determine the convergent series expressions of velocity , temperature and nanoparticle fraction. Graphs are plotted to provide the physical interpretation of different parameters.

3.1 Mathematical development

We consider the flow of nanofluid bounded by an exponentially stretching sheet . Surface is stretched along x -axis and y -axis is taken normal to x -axis. Along y -axis a uniform magnetic field of strength B_0 is applied. It is assumed that the induced magnetic field and the electric field effects are negligible. T_w and T_∞ are wall temperature and fluid temperature and C_w and C_∞ are wall concentration and concentration far away from the surface. The equations which govern the present flow situation with radiation and viscous dissipation effects are

$$\frac{\partial u}{\partial x} + \frac{\partial v}{\partial y} = 0, \quad (3.1)$$

$$u \frac{\partial u}{\partial x} + v \frac{\partial u}{\partial y} = \nu \frac{\partial^2 u}{\partial y^2} - \frac{\sigma B_0^2 u}{\rho_f}, \quad (3.2)$$

$$u \frac{\partial T}{\partial x} + v \frac{\partial T}{\partial y} = \alpha \frac{\partial^2 T}{\partial y^2} + \tau \left\{ D_B \frac{\partial C}{\partial y} \frac{\partial T}{\partial y} + \frac{D_T}{T_\infty} \left(\frac{\partial T}{\partial y} \right)^2 \right\} + \frac{\mu}{(\rho c)_f} \left(\frac{\partial u}{\partial y} \right)^2 + \frac{16\sigma^* T_\infty^3}{3k^*(\rho c)_f} \frac{\partial^2 T}{\partial y^2}, \quad (3.3)$$

$$u \frac{\partial C}{\partial x} + v \frac{\partial C}{\partial y} = D_B \frac{\partial^2 C}{\partial y^2} + \frac{D_T}{T_\infty} \frac{\partial^2 T}{\partial y^2}, \quad (3.4)$$

where u and v represents the velocity components along the x - and y - directions respectively, ρ_f denotes the fluid density, μ dynamic viscosity, ν the kinematic viscosity, p denotes the pressure, $(\rho c)_f$ the fluid heat capacity, $\tau = (\rho c)_p / (\rho c)_f$ the ratio parameter of nanoparticles heat capacity and fluid heat capacity with ρ being the density, D_B denotes the Brownian diffusion coefficient, D_T the thermophoretic diffusion coefficient, α the thermal diffusivity, σ the electrical conductivity of the base fluid, k^* represents the mean absorption coefficient and σ^* the Stefan-Boltzmann constant.

The subjected conditions are given as

$$\begin{aligned} u &= U_0 e^{\frac{x}{l}}, \quad v = 0, \quad T = T_w, \quad C = C_w \quad \text{at } y = 0, \\ u &= v = 0, \quad T \rightarrow T_\infty, \quad C \rightarrow C_\infty \quad \text{as } y \rightarrow \infty \end{aligned} \quad (3.5)$$

in which U_0 represents the reference velocity and l is a constant. Using the transformations

$$\begin{aligned} \varsigma &= y \sqrt{\frac{U_0}{2\nu l}} e^{\frac{x}{2l}}, \quad u = U_0 e^{\frac{x}{l}} F'(\varsigma), \quad v = -\sqrt{\frac{\nu U_0}{2l}} e^{\frac{x}{2l}} [F(\varsigma) + \varsigma F'(\varsigma)], \\ G(\varsigma) &= \frac{T - T_\infty}{T_w - T_\infty}, \quad J(\varsigma) = \frac{C - C_\infty}{C_w - C_\infty}, \end{aligned} \quad (3.6)$$

equation (3.1) is satisfied automatically and Eqs. (3.2) – (3.4) take the following form

$$F''' - 2F'^2 + FF'' - HrF' = 0, \quad (3.7)$$

$$\frac{1}{Pr} \left(1 + \frac{4}{3}R \right) G'' + FG' + BrJ'G' + TrG'^2 + EF''^2 = 0, \quad (3.8)$$

$$J'' + LFJ' + \frac{Tr}{Br} G'' = 0, \quad (3.9)$$

with

$$\begin{aligned} F(0) = 0, \quad F'(0) = 1, \quad G(0) = 1, \quad J(0) = 1, \\ F'(\infty) = 0, \quad G(\infty) = 0, \quad J(\infty) = 0, \end{aligned} \quad (3.10)$$

where prime indicates the differentiation with respect to ζ . Moreover the Prandtl number Pr , the Eckert number E , the radiation parameter R , the Lewis number L , the Hartman number Hr , the Brownian motion parameter Br and the thermophoresis parameter Tr are defined as

$$\begin{aligned} Pr = \frac{\nu}{\alpha}, \quad E = \frac{U_0^2 e^{\frac{2x}{l}}}{c_f(T_w - T_\infty)}, \quad R = \frac{4\sigma^* T_\infty^3}{k^* k}, \quad L = \frac{\nu}{D_B}, \\ Hr = \frac{2\sigma B_0^2 l}{\rho_f U_0} e^{-\frac{x}{l}}, \quad Br = \frac{(\rho c)_p D_B (C_w - C_\infty)}{(\rho c)_f \nu}, \quad Tr = \frac{(\rho c)_p D_T (T_w - T_\infty)}{(\rho c)_f T_\infty \nu}. \end{aligned} \quad (3.11)$$

The local skin friction C_f , Nusselt number Nu and the Sherwood number Sh are

$$C_f = \frac{\tau_w|_{y=0}}{\frac{1}{2}\rho U_0^2 e^{\frac{2x}{l}}}, \quad Nu = -\frac{x}{(T_w - T_\infty)} \frac{\partial T}{\partial y} \Big|_{y=0}, \quad Sh = -\frac{x}{D(C_w - C_\infty)} \frac{\partial C}{\partial y} \Big|_{y=0}, \quad (3.12)$$

$$C_f \sqrt{\frac{Re_x}{2}} = F''(0), \quad Nu Re_x^{-1/2} \sqrt{\frac{2l}{x}} = -G'(0), \quad Sh Re_x^{-1/2} \sqrt{\frac{2l}{x}} = -J'(0), \quad (3.13)$$

where $Re_x = U_0 e^{\frac{x}{l}} x / \nu$ is the local Reynolds number.

3.2 Homotopy solution

Initial approximations and auxiliary linear operators are defined as

$$F_0(\zeta) = 1 - e^{-\zeta}, \quad G_0(\zeta) = e^{-\zeta}, \quad J_0(\zeta) = e^{-\zeta}, \quad (3.14)$$

$$\mathcal{L}_F = F''' - F', \quad \mathcal{L}_G = G'' - G, \quad \mathcal{L}_J = J'' - J. \quad (3.15)$$

The above operators satisfy

$$\mathcal{L}_F(A_1 + A_2 e^\zeta + A_3 e^{-\zeta}) = 0, \quad (3.16)$$

$$\mathcal{L}_G(A_4 e^\zeta + A_5 e^{-\zeta}) = 0, \quad (3.17)$$

$$\mathcal{L}_J(A_6e^\varsigma + A_7e^{-\varsigma}) = 0, \quad (3.18)$$

where A_n ($n = 1 - 7$) are the arbitrary constants.

3.2.1 Zeroth order deformation equations

Let $w \in [0, 1]$ denotes an embedding parameter, \hbar_F , \hbar_G and \hbar_J are the non-zero convergence control parameters then we construct the following zeroth-order deformation problems:

$$(1 - w) \mathcal{L}_F [\widehat{F}(\varsigma; w) - F_0(w)] = w \hbar_F \mathcal{N}_F [\widehat{F}(\varsigma; w)], \quad (3.19)$$

$$\widehat{F}(0; w) = 0, \quad \widehat{F}'(0; w) = 1, \quad \widehat{F}'(\infty; w) = 0, \quad (3.20)$$

$$(1 - w) \mathcal{L}_G [\widehat{G}(\varsigma; w) - G_0(w)] = w \hbar_G \mathcal{N}_G [\widehat{G}(\varsigma; w)], \quad (3.21)$$

$$\widehat{G}(0; w) = 1, \quad \widehat{G}(\infty; w) = 0, \quad (3.22)$$

$$(1 - w) \mathcal{L}_J [\widehat{J}(\varsigma; w) - J_0(w)] = w \hbar_J \mathcal{N}_J [\widehat{J}(\varsigma; w)], \quad (3.23)$$

$$\widehat{J}(0; w) = 1, \quad \widehat{J}(\infty; w) = 0, \quad (3.24)$$

in which prime indicates differentiation with respect to ς and the non-linear operator $\mathcal{N}_F [\widehat{F}(\varsigma; w)]$, $\mathcal{N}_G [\widehat{G}(\varsigma; w)]$ and $\mathcal{N}_J [\widehat{J}(\varsigma; w)]$ of Eqs. (3.7) – (3.9) are

$$\mathcal{N}_F [\widehat{F}(\varsigma; w)] = \frac{\partial^3 \widehat{F}(\varsigma; w)}{\partial \varsigma^3} - 2 \left(\frac{\partial \widehat{F}(\varsigma; w)}{\partial \varsigma} \right)^2 + \widehat{F}(\varsigma; w) \frac{\partial^2 \widehat{F}(\varsigma; w)}{\partial \varsigma^2} - Hr \frac{\partial \widehat{F}(\varsigma; w)}{\partial \varsigma}, \quad (3.25)$$

$$\begin{aligned} \mathcal{N}_G [\widehat{G}(\varsigma; w)] &= \frac{1}{Pr} \left(1 + \frac{4}{3}R \right) \frac{\partial^2 \widehat{G}(\varsigma; w)}{\partial \varsigma^2} + \widehat{F}(\varsigma; w) \frac{\partial \widehat{G}(\varsigma; w)}{\partial \varsigma} + Br \frac{\partial \widehat{G}(\varsigma; w)}{\partial \varsigma} \frac{\partial \widehat{J}(\varsigma; w)}{\partial \varsigma} \\ &+ Tr \left(\frac{\partial \widehat{G}(\varsigma; w)}{\partial \varsigma} \right)^2 + E \left(\frac{\partial^2 \widehat{F}(\varsigma; w)}{\partial \varsigma^2} \right)^2, \end{aligned} \quad (3.26)$$

$$\mathcal{N}_J [\widehat{J}(\varsigma; w)] = \frac{\partial^2 \widehat{J}(\varsigma; w)}{\partial \varsigma^2} + L \widehat{F}(\varsigma; w) \frac{\partial \widehat{J}(\varsigma; w)}{\partial \varsigma} + \frac{Tr}{Br} \frac{\partial^2 \widehat{G}(\varsigma; w)}{\partial \varsigma^2}, \quad (3.27)$$

As w increases from 0 to 1, $\widehat{F}(\varsigma, w)$, $\widehat{G}(\varsigma, w)$ and $\widehat{J}(\varsigma, w)$ varies continuously from initial guesses $F_0(\varsigma)$, $G_0(\varsigma)$ and $J_0(\varsigma)$ to the final solution $F(\varsigma)$, $G(\varsigma)$ and $J(\varsigma)$. For $w = 0$ and $w = 1$, one respectively has

$$\widehat{F}(\varsigma, 0) = F_0(\varsigma), \quad \widehat{F}(\varsigma, 1) = F(\varsigma), \quad (3.28)$$

$$\widehat{G}(\varsigma, 0) = G_0(\varsigma), \quad \widehat{G}(\varsigma, 1) = G(\varsigma), \quad (3.29)$$

$$\widehat{J}(\varsigma, 0) = J_0(\varsigma), \quad \widehat{J}(\varsigma, 1) = J(\varsigma). \quad (3.30)$$

Expanding $\widehat{F}(\varsigma, w)$, $\widehat{G}(\varsigma, w)$ and $\widehat{J}(\varsigma, w)$ in power series of the embedding parameter w as:

$$\widehat{F}(\varsigma, w) = F_0(\varsigma) + \sum_{m=1}^{\infty} F_m(\varsigma)w^m; \quad F_m(\varsigma) = \left. \frac{1}{m!} \frac{\partial^m \widehat{F}(\varsigma, w)}{\partial w^m} \right|_{w=0}, \quad (3.31)$$

$$\widehat{G}(\varsigma, w) = G_0(\varsigma) + \sum_{m=1}^{\infty} G_m(\varsigma)w^m; \quad G_m(\varsigma) = \left. \frac{1}{m!} \frac{\partial^m \widehat{G}(\varsigma, w)}{\partial w^m} \right|_{w=0}, \quad (3.32)$$

$$\widehat{J}(\varsigma, w) = J_0(\varsigma) + \sum_{m=1}^{\infty} J_m(\varsigma)w^m; \quad J_m(\varsigma) = \left. \frac{1}{m!} \frac{\partial^m \widehat{J}(\varsigma, w)}{\partial w^m} \right|_{w=0}, \quad (3.33)$$

where the convergence of series (3.31) – (3.33) depends upon \hbar_F , \hbar_G and \hbar_J . We select the parameters \hbar_F , \hbar_G and \hbar_J such that the series converge at $w = 1$, then by Eqs. (3.28) – (3.30), we get

$$F(\varsigma) = F_0(\varsigma) + \sum_{m=1}^{\infty} F_m(\varsigma), \quad (3.34)$$

$$G(\eta) = G_0(\varsigma) + \sum_{m=1}^{\infty} G_m(\varsigma), \quad (3.35)$$

$$J(\eta) = J_0(\varsigma) + \sum_{m=1}^{\infty} J_m(\varsigma). \quad (3.36)$$

3.2.2 Problems at mth-order deformation

Taking the derivative of zeroth order deformation Eqs. (3.19) – (3.24) m times with respect to w then setting $w = 0$, we have

$$\mathcal{L}_F [F_m(\varsigma) - \chi_m F_{m-1}(\varsigma)] = \hbar_F \mathcal{R}_m^F(\varsigma), \quad (3.37)$$

$$F_m(0) = F'_m(0) = F'_m(\infty) = 0, \quad (3.38)$$

$$\mathcal{L}_G [G_m(\varsigma) - \chi_m G_{m-1}(\varsigma)] = \hbar_G \mathcal{R}_m^G(\varsigma), \quad (3.39)$$

$$G_m(0) = G_m(\infty) = 0, \quad (3.40)$$

$$\mathcal{L}_J [J_m(\varsigma) - \chi_m J_{m-1}(\varsigma)] = \hbar_J \mathcal{R}_m^J(\varsigma), \quad (3.41)$$

$$J_m(0) = J_m(\infty) = 0, \quad (3.42)$$

in which

$$\mathcal{R}_m^F(\varsigma) = \left[F'''_{m-1} - 2 \sum_{i=0}^{m-1} F'_{m-1-i} F'_i + \sum_{i=0}^{m-1} F_{m-1-i} F''_i - Hr F'_{m-1} \right], \quad (3.43)$$

$$\mathcal{R}_m^G(\varsigma) = \frac{1}{Pr} \left(1 + \frac{4}{3} R \right) G''_{m-1} + \sum_{i=0}^{m-1} [F_{m-1-i} G'_i + Br G'_{m-1-i} J'_i + Tr G'_{m-1-i} G'_i + E F''_{m-1-i} F''_i], \quad (3.44)$$

$$\mathcal{R}_m^J(\varsigma) = \left[J''_{m-1} + L \sum_{i=0}^{m-1} F_{m-1-i} J'_i + \frac{Tr}{Br} G''_{m-1} \right], \quad (3.45)$$

$$\chi_m = \begin{cases} 0, & m \leq 1 \\ 1, & m > 1 \end{cases}, \quad (3.46)$$

and the general solutions are

$$F_m(\varsigma) = F_m^*(\varsigma) + A_1 + A_2 e^\varsigma + A_3 e^{-\varsigma}, \quad (3.47)$$

$$G_m(\varsigma) = G_m^*(\varsigma) + A_4 e^\varsigma + A_5 e^{-\varsigma}, \quad (3.48)$$

$$J_m(\varsigma) = J_m^*(\varsigma) + A_6 e^\varsigma + A_7 e^{-\varsigma}, \quad (3.49)$$

where F_m^* , G_m^* and J_m^* are the particular solutions and the constants A_n ($n = 1 - 7$) along with the boundary conditions (3.38), (3.40) and (3.42) are

$$\begin{aligned} A_1 &= -F_m^*(0) - A_3, \quad A_2 = A_4 = A_6 = 0, \quad A_3 = \left. \frac{\partial F_m^*(\varsigma)}{\partial \varsigma} \right|_{\varsigma=0}, \\ A_5 &= -G_m^*(0), \quad A_7 = -J_m^*(0). \end{aligned} \quad (3.50)$$

3.3 Convergence of HAM solution

Now the solution of Eqs. (3.7) – (3.9) with the boundary conditions (3.10) is computed using homotopy analysis method. We choose auxiliary parameters \hbar_F , \hbar_G and \hbar_J for the functions F , G and J respectively. The values of non-zero auxiliary parameters have a key role in the convergence of series expression. The \hbar -curves are plotted in Figs. (3.1 and 3.2). The range of admissible values of \hbar for F is $-1.05 \leq \hbar_F \leq -0.35$, for G is $-1.2 \leq \hbar_G \leq -0.6$ and similarly for J is $-1.1 \leq \hbar_J \leq -0.8$. It is also evident from Figs. (3.1 and 3.2) that series solutions converge in the whole region of ς ($0 < \varsigma < \infty$) for \hbar_F , \hbar_G and $\hbar_J = -0.9$.

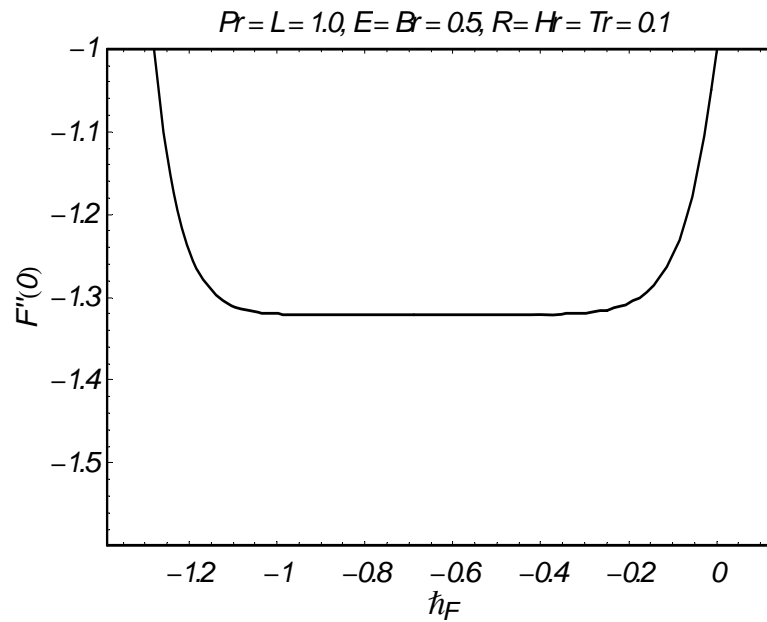


Fig. 3.1: \hbar -curves for F .

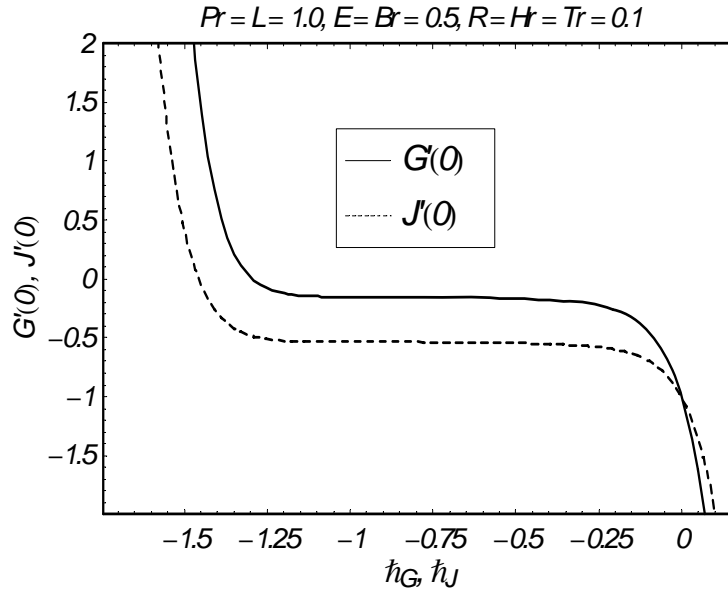


Fig. 3.2: h -curves for G and J .

Table 3.1. Convergence of HAM solutions for different order of approximations when $Pr = 1.0 = L$, $E = Br = 0.5$ and $R = Tr = Hr = 0.1$.

Order of approximations	$-F''(0)$	$-G'(0)$	$-J'(0)$
1	1.34500	0.310000	0.610000
5	1.32244	0.173634	0.550958
10	1.32091	0.155242	0.536540
15	1.32103	0.152030	0.533693
20	1.32101	0.151226	0.532938
25	1.32101	0.151002	0.532715
30	1.32101	0.150934	0.532645
35	1.32101	0.150913	0.532622
40	1.32101	0.150906	0.532614
46	1.32101	0.150903	0.532611
50	1.32101	0.150903	0.532611
60	1.32101	0.150903	0.532611

3.4 Results and discussion

Here Figs. (3.3 – 3.17) are plotted for the effects of various parameters on the velocity, temperature and mass fraction fields. Fig. 3.3 displays the effect of Hartman number Hr on F' . The velocity field F' is found to decrease when Hr increases. Effects of Prandtl number Pr , Hartman number Hr , Eckert number E , radiation parameter R , Brownian motion parameter Br , thermophoresis parameter Tr and Lewis number L on the temperature profile G and the mass fraction field J are shown in the Figs. (3.4 – 3.17), respectively. It is noted that by increasing the Prandtl number, decreases the temperature profile G and increases the boundary layer thickness. Infact the thermal diffusivity decreases by increasing Pr and thus the heat diffused away slowly from the heated surface. It is found that G increases when Hr increases. The influence of E on the temperature profile G is shown in Fig. 3.6. It is noted that G and thermal boundary layer increases by increasing E . The effect of R on G and thermal boundary layer thickness is same as that of E . Further, the temperature profile G and thermal boundary layer increase when Br and Tr are increased. Also the temperature profile G and thermal boundary layer thickness decrease when the Lewis number L increases. This is due to the fact that an increase in the L reduces the molecular diffusivity. It is observed that the mass fraction field J and the associated boundary layer increase when the Prandtl number Pr and thermophoresis parameter Tr increases, whereas it decrease when Hartman number Hr , Eckert number E , radiation number R , Brownian motion parameter Br and Lewis number L are increased.

Figs. (3.18 – 3.21) illustrates the change in dimensionless heat and mass transfer rates vs Tr parameter. Here the effects of Pr , L , and Br on the dimensionless heat and mass transfer rates are shown for the same Hr , E and R . Obviously the dimensionless heat transfer rates decrease with an increase in Pr number. Fig. 3.19 shows that the dimensionless heat transfer rates decrease by increasing Br for small L number. However, for larger value of L number, the dimensionless heat transfer rates increase with an increase in Br . It is clear from Fig. 3.20 that the dimensionless mass transfer rates increase with the increase in Pr . The increase in dimensionless mass transfer rates is monotonic for larger L .

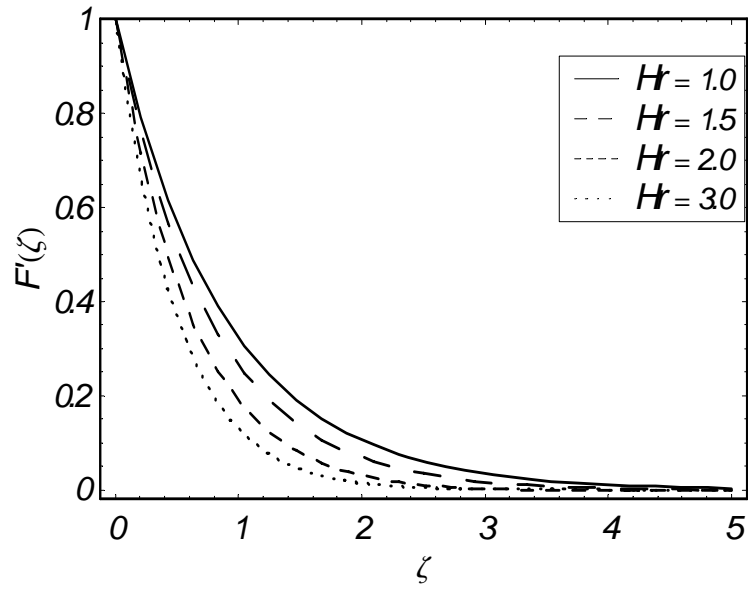


Fig. 3.3: Influence of Hr on F' .

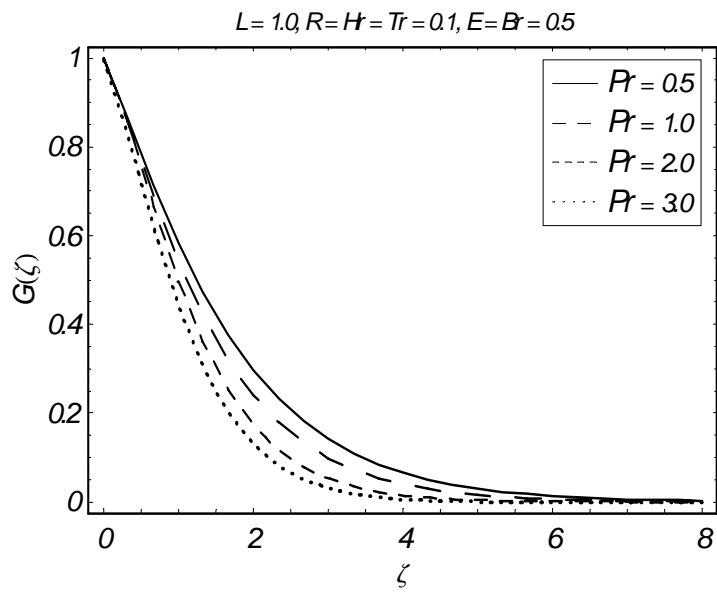


Fig. 3.4: Influence of Pr on G .

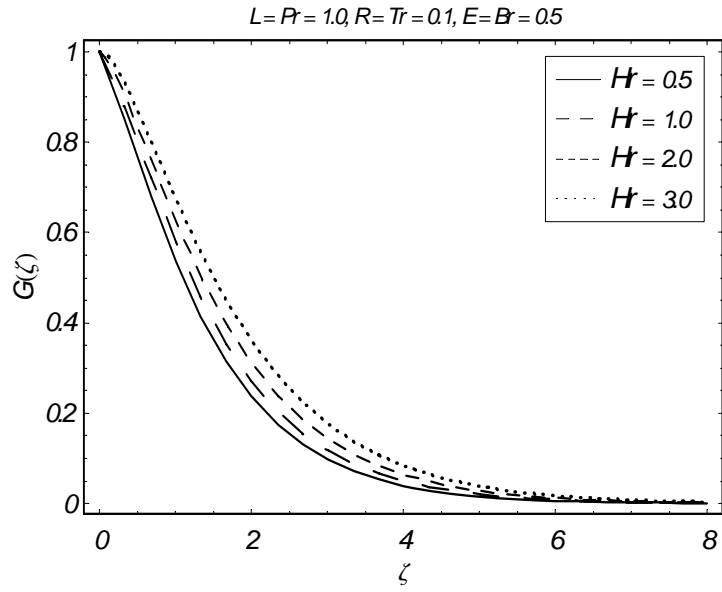


Fig. 3.5: Influence of Hr on G .

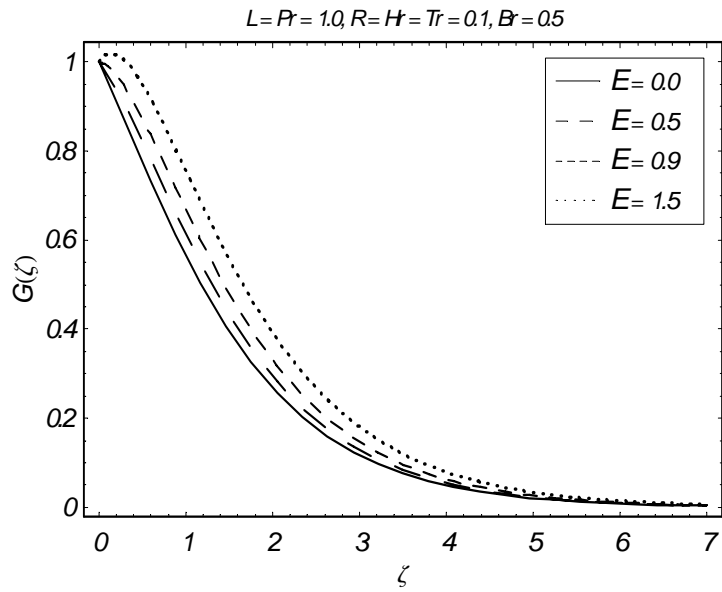


Fig. 3.6: Influence of E on G .

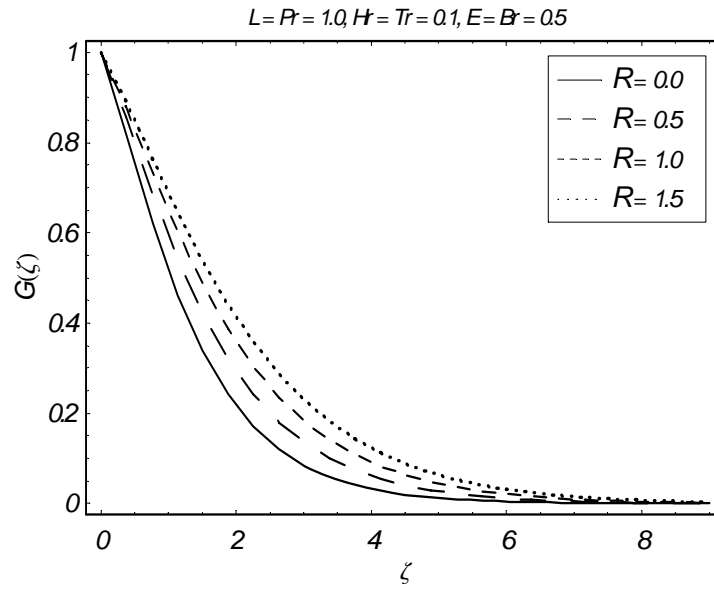


Fig. 3.7: Influence of R on G .

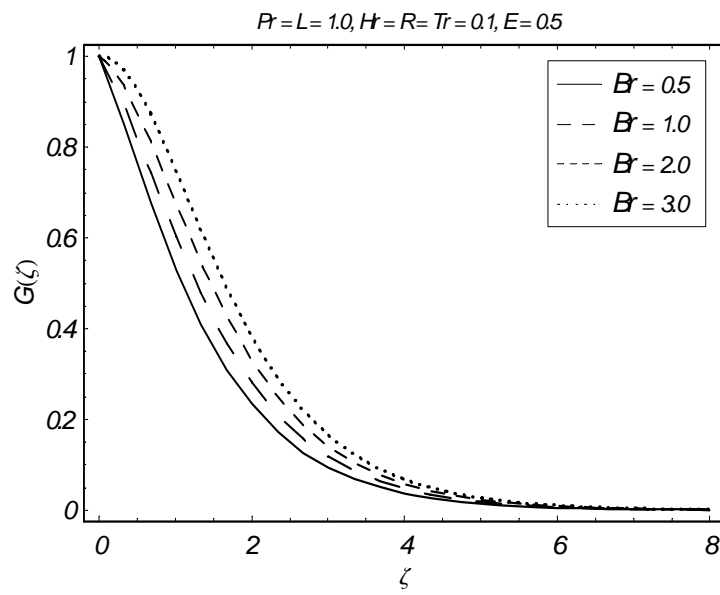


Fig. 3.8: Influence of Br on G .

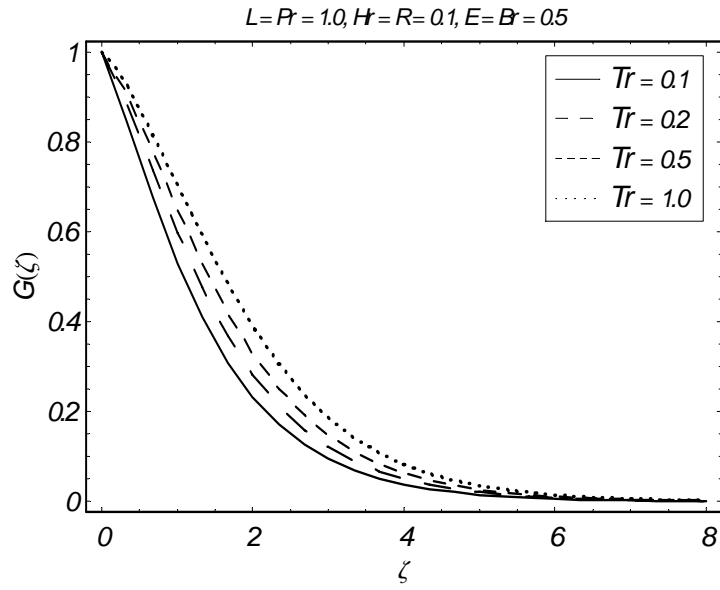


Fig. 3.9: Influence of Tr on G .

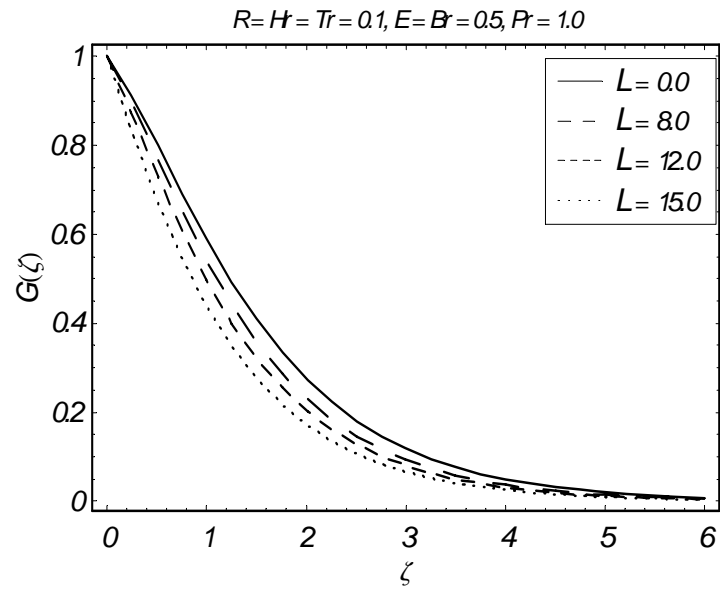


Fig. 3.10: Influence of L on G .

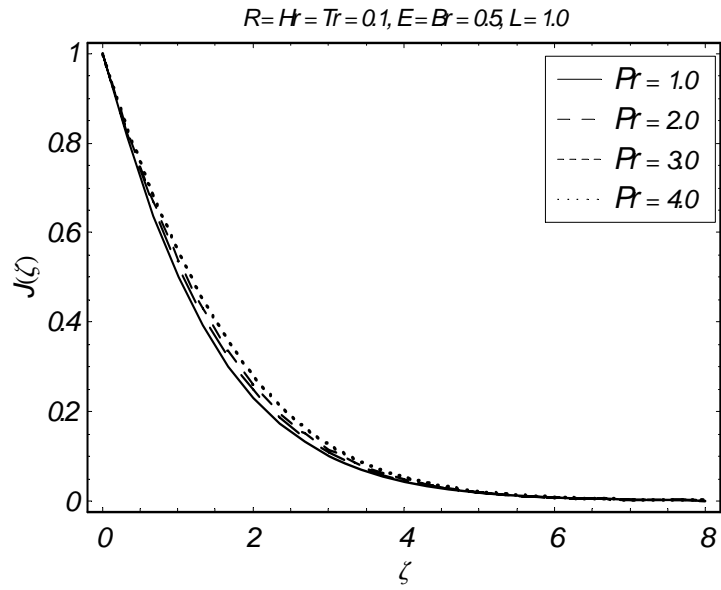


Fig. 3.11: Influence of Pr on J .

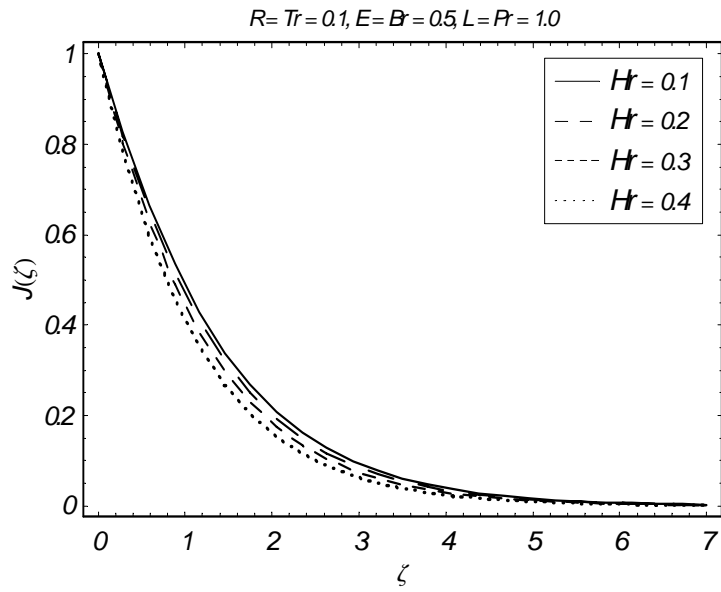


Fig. 3.12: Influence of Hr on J .

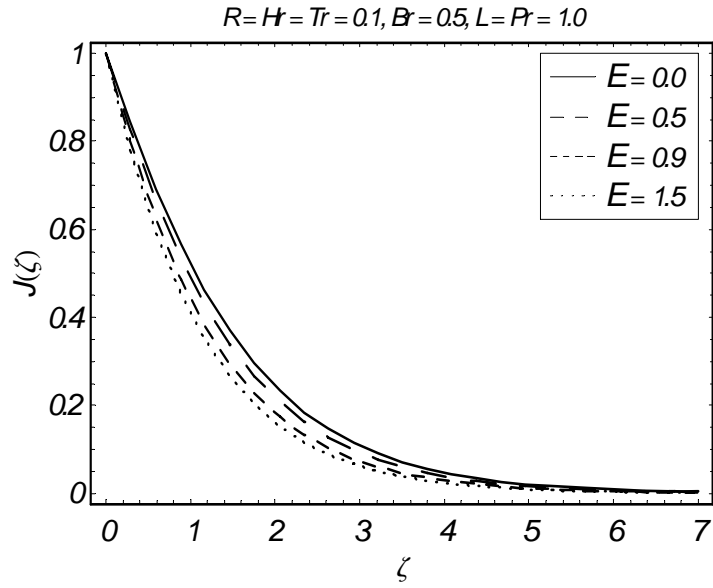


Fig. 3.13: Influence of E on J .

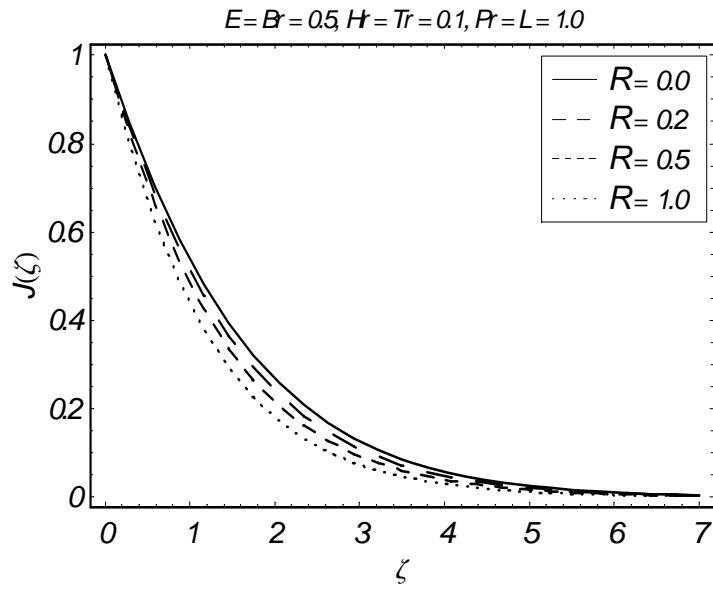


Fig. 3.14: Influence of R on J .

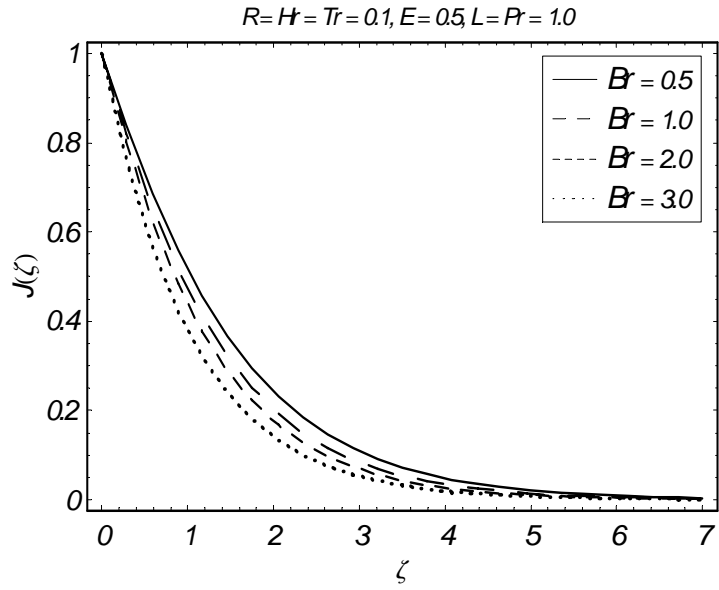


Fig. 3.15: Influence of Br on J .

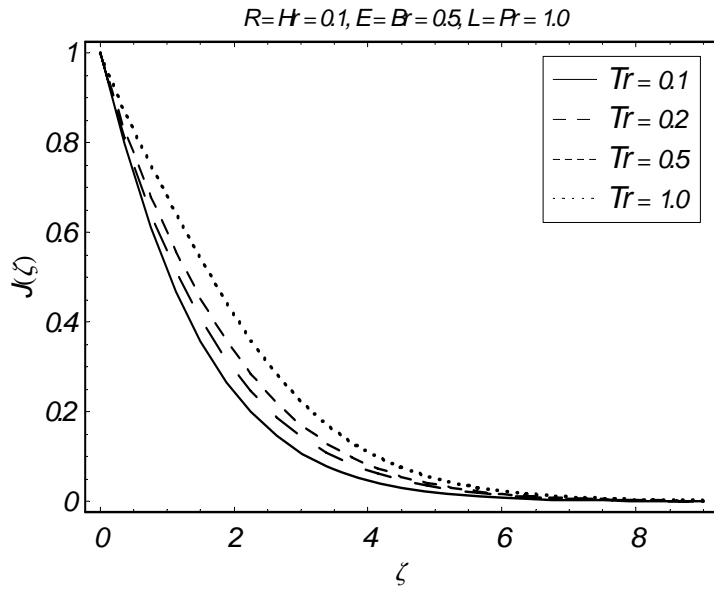


Fig. 3.16: Influence of Tr on J .

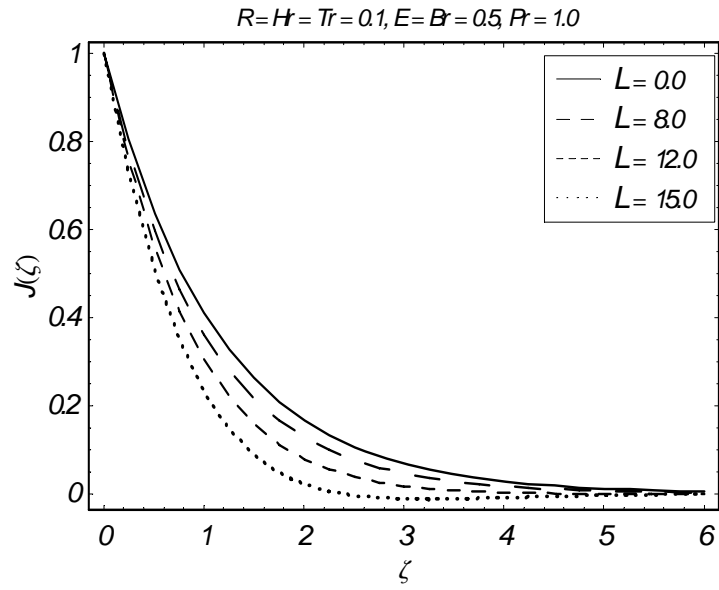
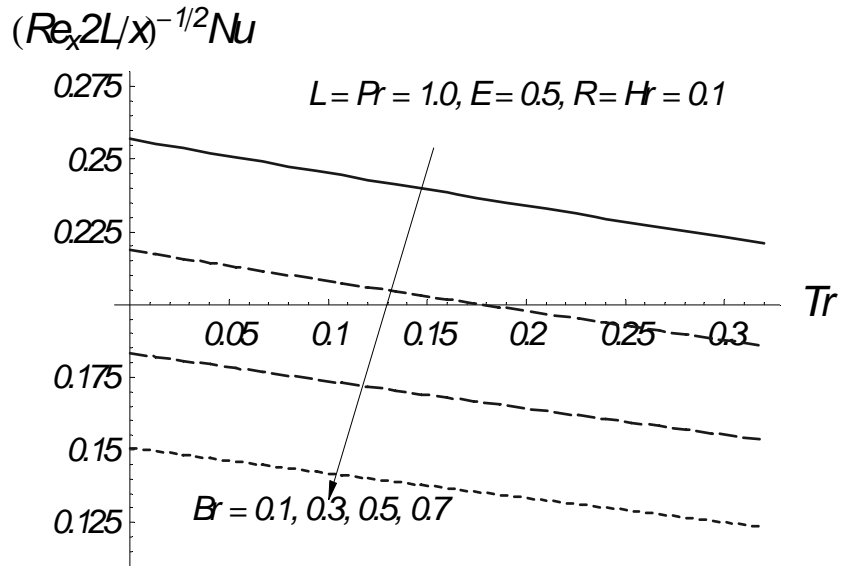
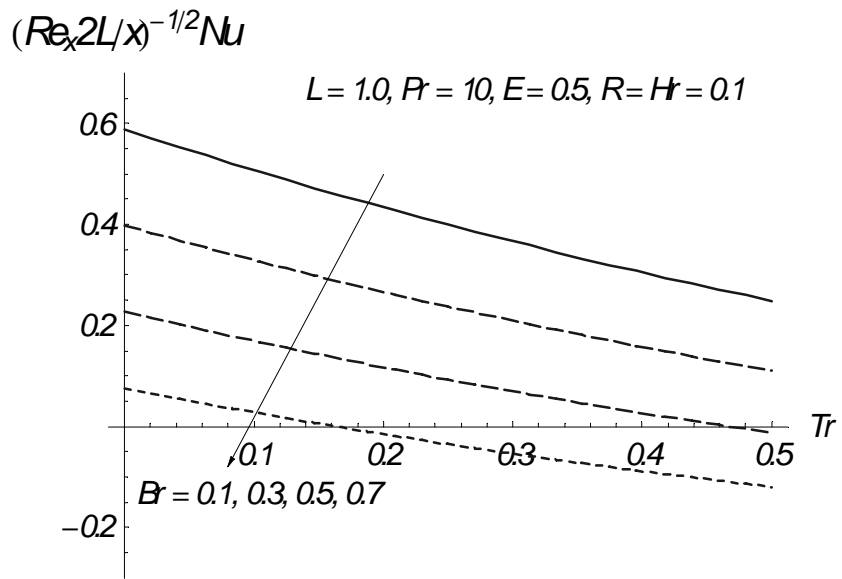


Fig. 3.17: Influence of L on J .



(a)



(b)

Fig. 3.18: Effects of Br and Pr on dimensionless heat transfer rates.

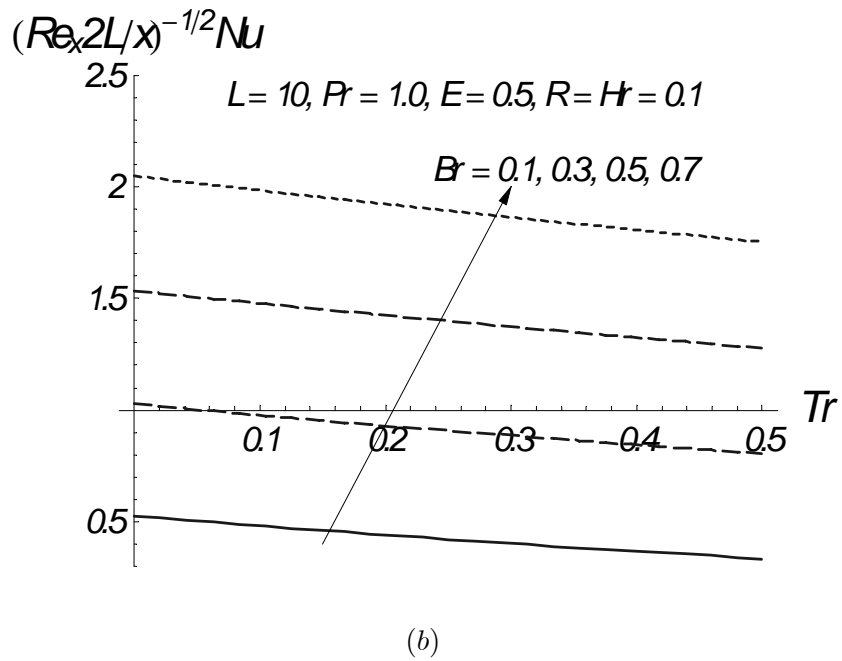
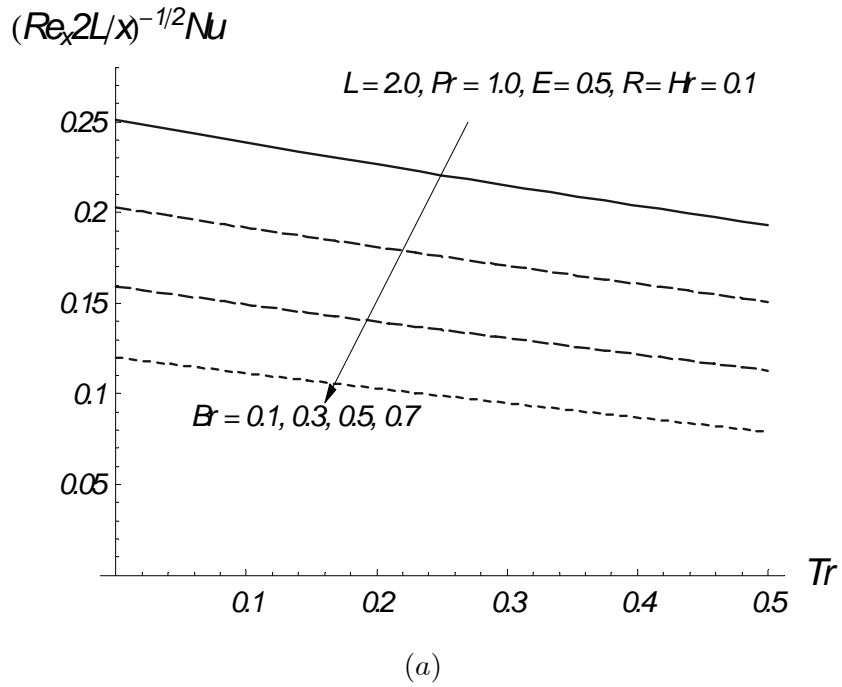
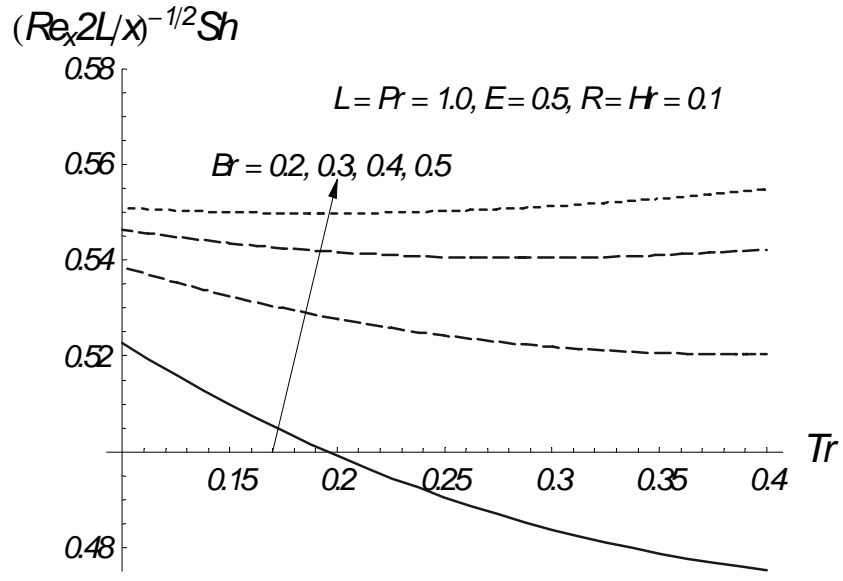
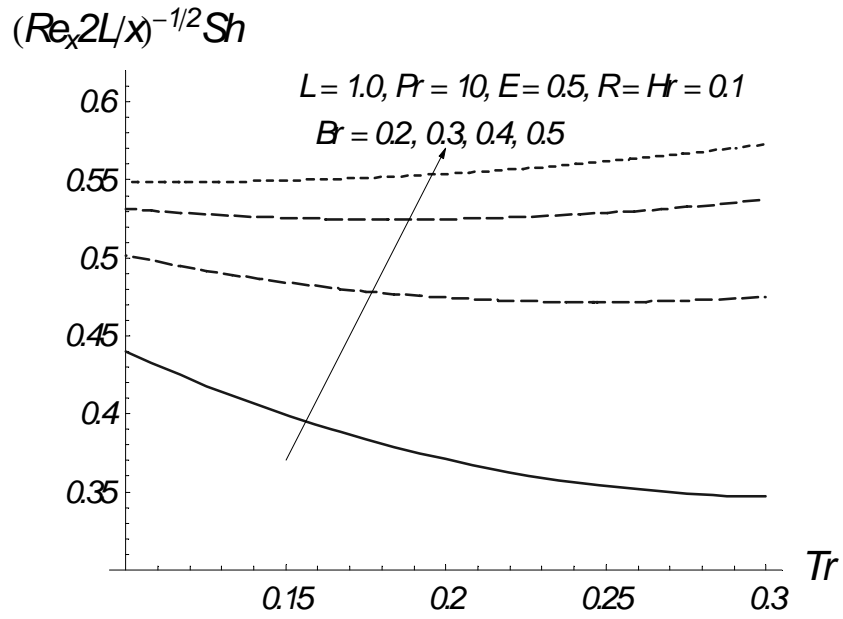


Fig. 3.19: Effects of Br and L on dimensionless heat transfer rates.



(a)



(b)

Fig. 3.20: Effects of Br and Pr on dimensionless concentration rates.

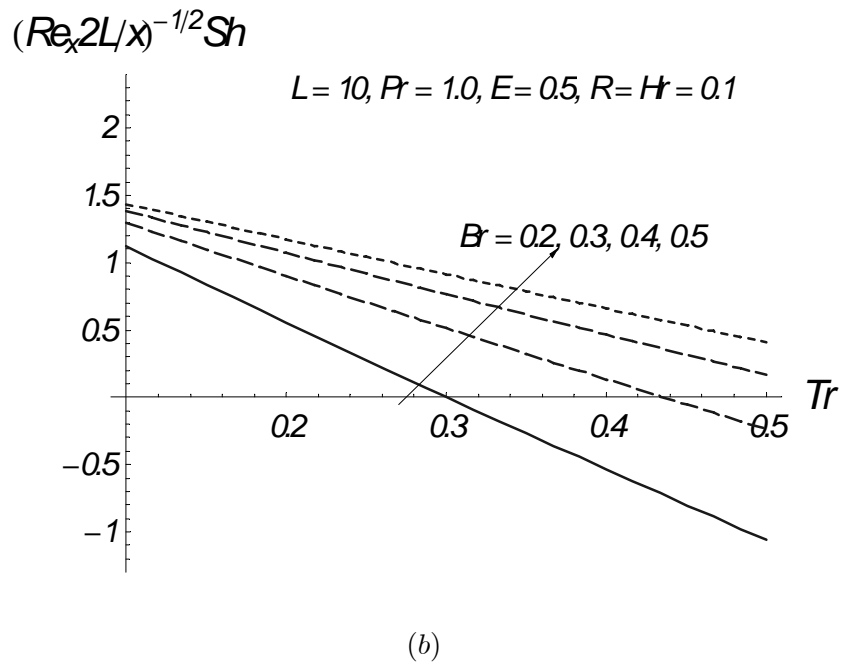
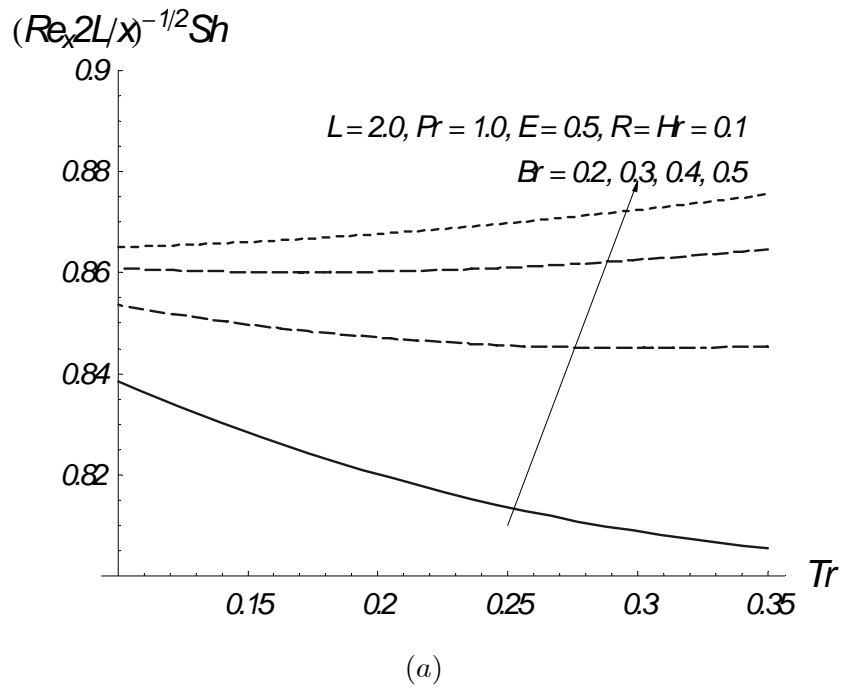


Fig. 3.21: Effects of Br and L on dimensionless concentration rates.

3.5 Concluding remarks

Magnetohydrodynamic (MHD) nanofluid flow on an exponentially stretching sheet is discussed. Few interesting findings of the present study are as follows:

- The velocity profile F' decreases by increasing Hartman number Hr .
- Increase in the Prandtl number Pr and the Lewis number L decreases the temperature and boundary layer thickness.
- Effects of the Hartman number Hr , the Eckert number E , the radiation parameter R , the Brownian motion parameter Br and thermophoresis parameter Tr on the temperature and thermal boundary layer thickness are quite opposite to that of Pr and L .
- An increase in the Hartman number Hr , Eckert number E , radiation parameter R , Brownian motion parameter Br , and Lewis number L reduces the mass fraction field J and the boundary layer thickness. By increasing Prandtl number Pr and thermophoresis parameter Tr , J increases.
- Reduced Nusselt number is a decreasing function of Pr , an increasing function of lower L and decreasing function of higher L while the reduced Sherwood number is an increasing function.

Bibliography

- [1] B. C. Sakiadis, Boundary-layer behavior on continuous solid surfaces. I. Boundary-layer equations for two-dimensional and axisymmetric flow, *AIChE J* 7 (1961) 26 – 28.
- [2] L. J. Crane, Flow past a stretching plate, *Zeitschrift Fur Angewandte Mathematik Und Physik* 7 (1961) 21 – 28.
- [3] K. R. Rajagopal, T. Y. Na and A. S. Gupta, Flow of a viscoelastic fluid over a stretching sheet, *Rheol. Acta* 23 (1984) 213 – 215.
- [4] K. Sankara and L. T. Watson, Micropolar fluid past a stretching sheet, *Z. Angew. Math. Phys.* 36 (1985) 845 – 853.
- [5] H. I. Andersson, K. H. Bech and B. S. Dandapat, Magnetohydrodynamic flow of powerlaw fluid over a stretching sheet, *Int. J. Nonlinear Mech.* 27 (1992) 929 – 936.
- [6] T. R. Mahapatra and A. S. Gupta, Stagnation-point flow of a viscoelastic fluid towards a stretching surface, *Int. J. Nonlinear Mech.* 39 (2004) 811 – 820.
- [7] R. Cortell, MHD flow and mass transfer of an electrically conducting fluid of second grade in a porous medium over a stretching sheet with chemically reactive species, *Chem. Eng. Process* 46 (2007) 721 – 728.
- [8] N. Bachok, A. Ishak and I. Pop, Melting heat transfer in boundary layer stagnation point flow towards a stretching/shrinking sheet, *Phys. Lett. A*, 374 (2010) 4075 – 4079.
- [9] N. A. Yacob, A. Ishak and I. Pop, Melting heat transfer in boundary layer stagnation-point flow towards a stretching/shrinking sheet in a micropolar fluid, *Comp. Fluids*, 47 (2011) 16 – 21.

- [10] M. Mustafa, T. Hayat, I. Pop, S. Asghar and S. Obaidat, Stagnation-point flow of a nanofluid towards a stretching sheet, *Int. J. Heat Mass Transfer* 54 (2011) 5588 – 5594.
- [11] T. Hayat, M. Mustafa, S. A. Shehzad and S. Obaidat, Melting heat transfer in the stagnation-point flow of an upper-convected Maxwell (UCM) fluid past a stretching sheet, *Int. J. Num. Meth. fluids* DOI: 10.1002/fld.2503.
- [12] E. Magyari and B. Keller, Heat and mass transfer in the boundary layers on an exponentially stretching continuous surface, *J. Phys.: D. Appl. Phys.* 32 (1999) 577 – 585.
- [13] E.M.A. Elbashbeshy, Heat transfer over an exponentially stretching continuous surface with suction, *Arch Mech.* 53 (2001) 643 – 651.
- [14] S. K. Khan and Sanjayanand, Viscoelastic boundary layer flow and heat transfer over an exponential stretching sheet, *Int. J. Heat Mass Transfer* 48 (2005) 1534 – 1542.
- [15] M. Sajid and T. Hayat, Influence of thermal radiation on the boundary layer flow due to an exponentially stretching sheet. *Int comm. Heat Mass Transfer* 35 (2008) 347 – 356.
- [16] S.U.S. Choi, Enhancing thermal conductivity of fluids with nanoparticle, in: D.A. Siginer, H.P. Wang (eds.), *Developments and Applications of Non-Newtonian Flows*, ASME FED, 231 (1995) 99 – 105.
- [17] A.V. Kuznetsov and D.A. Nield, Natural convective boundary-layer flow of a nanofluid past a vertical plate, *Int. J. Thermal Sci.* 49 (2010) 243 – 247.
- [18] D.A. Nield and A.V. Kuznetsov, The Cheng–Minkowycz problem for natural convective boundary-layer flow in a porous medium saturated by a nanofluid, *Int. J. Heat Mass Transfer* 52 (2009) 5792 – 5795.
- [19] W. A. Khan and I. Pop, Boundary-layer flow of a nanofluid past a stretching sheet, *Int. J. Heat Mass Transfer* 53 (2010) 2477 – 2483.
- [20] P. Rana and R. Bhargava, Flow and heat transfer of a nanofluid over a nonlinearly stretching sheet: A numerical study, *Comm. Nonlinear Sci. Num. Simul.* DOI: 10.1016/j.cnsns.2011.05.009.

- [21] O. Makinde and A. Aziz, Boundary layer flow of a nanofluid past a stretching sheet with a convective boundary condition, *Int. J. Therm. Sci.* 50 (2011) 1326 – 1332.
- [22] S. Nadeem and C. Lee, Boundary layer flow of nanofluid over an exponentially stretching surface, *Nanoscale Res. Lett.* (2012), 7 : 94.
- [23] S. J. Liao, *Beyond Perturbation: Introduction to Homotopy Analysis Method*, Chapman and Hall/CRC Press, Boca Raton (2003).
- [24] S. J. Liao, A new branch of solutions of boundary-layer flows over an impermeable stretched plate, *Int. J. Heat Mass Transfer* 48 (2005) 2529 – 2539.
- [25] S. Abbasbandy and A. Shirzadi, A new application of the homotopy analysis method: Solving the Sturm–Liouville problems, *Comm. Non-linear Sci. Num. Simul.* 16 (2011) 112–126.
- [26] S. Abbasbandy, The application of homotopy analysis method to nonlinear equations arising in heat transfer, *Phys. Lett. A*, 360 (2006) 109 – 113.
- [27] A. S. Bataineh, M.S.M. Noorani and I. Hashim, On a new reliable modification of homotopy analysis method, *Comm. Non-linear Sci. Num. Simul.* 14 (2009) 409 – 423.
- [28] T. Hayat, Z. Iqbal, M. Qasim, S. Obaidat, Steady flow of an Eyring Powell fluid over a moving surface with convective boundary conditions, *Int. J. Heat Mass Transfer* 55 (2012) 1817 – 1822.
- [29] T. Hayat, M. Qasim and Z. Abbas, Three-dimensional flow of an elastico-viscous fluid with mass transfer, *Int. J. Num. Methods in Fluids* 66 (2011) 194 – 211.
- [30] T. Hayat and M. Awais, Simultaneous effects of heat and mass transfer on time-dependent flow over a stretching surface, *Int. J. Num. Methods in Fluids*, 67 (2011) 1341 – 1357.
- [31] T. Hayat, M. Mustafa and A. A. Hendi, Time-dependent three-dimensional flow and mass transfer of elastico-viscous fluid over unsteady stretching sheet, *Appl. Math. Mech.* 32 (2011) 167 – 178.